

Figure 4. Blood biochemistry of 15-week-old mice, exposed to 2,3,7,8-tetrachlorodibenzo-*p*-dioxin (TCDD) *in utero* and via lactation, that were fed a high-calorie diet or a regular diet after weaning. Total cholesterol (A), triglyceride (B), high-density lipoprotein cholesterol (HDLC) (C) and AST (C) in serum were determined using Fuji Dri-Chem 7000 V. Data are shown as the mean \pm SE ($n=6-7$ per group). Differences in means were analyzed by two-way ANOVA with a post hoc test. Overall, significant main effects of diet were found in (A) and (C). See *P*-values in the 'Results'. No statistical comparison was performed between the V-R and T-H groups, or between the T-R and V-H groups.

product purity. The expression levels of mRNAs of target genes were calculated by the ΔC_t method using *CypB* for normalization.

Statistical Analysis

Data were analyzed on a litter-by-litter basis. SPSS for Windows version 15.0 (SPSS Japan Inc., Tokyo, Japan) was used for the statistical analysis. All data are shown as the mean \pm the standard error (SE) of the mean. Differences in means were analyzed by two-way analysis of variance (ANOVA) followed by Tukey's honestly significant difference (HSD) test for post hoc analysis. Unless otherwise stated, no significant interactions between diet (regular diet or high calorie diet) and exposure (dioxin or vehicle) were observed. A *P*-value of less than 0.05 was considered statistically significant.

Results

Body Weight and Blood Pressure

The body weight was not different among the four groups (V-R, V-H, T-R and T-H) at PND 28. The body weight of mouse offspring given a high-calorie diet (V-H and T-H groups) was significantly increased during the entire experimental period (Fig. 1A, $P < 0.05$). A significant main effect of diet at week 15 [$F(1,23) = 16.7$, $P < 0.001$] and at week 26 [$F(1,24) = 214$, $P < 0.001$] was observed on liver weight, but no significant main effect of exposure was observed (Fig. 1B).

No alterations by the type of diet or by TCDD exposure were found for the mean systolic blood pressure at 9, 19 or 23 weeks after birth (Table 2). For example, the systolic blood pressure values (mean \pm SE) of 23-week-old mice in the V-R, T-R, V-H and T-H groups were 116 ± 2 , 122 ± 2 , 125 ± 4 and 125 ± 4 mmHg, respectively. No difference in the pulse rate was found between the groups during the blood pressure measurement.

Effect of TCDD Exposure on CYP1A1 and CYP1A2 mRNA Levels

To examine whether TCDD had direct effects on the mice at 15 weeks of age, mRNA levels of the indicator genes of TCDD exposure, CYP1A1 and 1A2, were measured in the liver (Fig. 2). No significant main effect of exposure was revealed as assessed by CYP1A1 mRNA abundance, but a significant main effect of diet [$F(1,15) = 5.74$, $P < 0.05$] was found by two-way ANOVA. In contrast, CYP1A2 mRNA abundance revealed a significant main effect of exposure [$F(1,15) = 6.48$, $P < 0.05$], as well as a significant main effect of diet [$F(1,15) = 42.9$, $P < 0.001$]. In addition, there was a significant difference between the V-R and V-H groups ($P < 0.001$) and the T-R and T-H groups ($P < 0.001$), whereas no significant differences were observed between the V-R and T-R groups and the V-H and T-H groups. These results suggest that nearly all of the TCDD was eliminated from the body by week 15 after birth, probably owing to the fact that the elimination half-life of TCDD is approximately 11 days in C57Bl/6 mice (Gasiewicz et al., 1983).

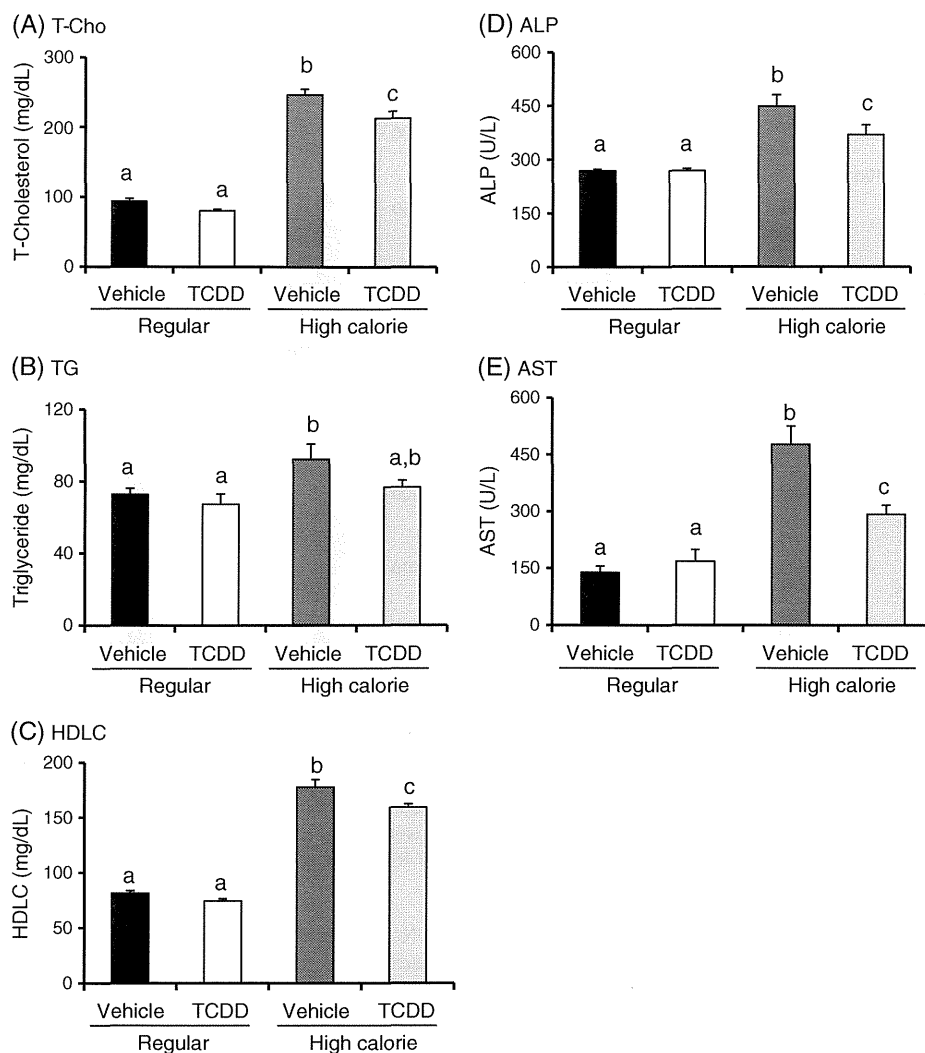


Figure 5. Blood biochemistry of 26-week-old mice, exposed to 2,3,7,8-tetrachlorodibenzo-*p*-dioxin (TCDD) *in utero* and via lactation, that were fed a high-calorie diet or a regular diet after weaning. Total cholesterol (A), triglyceride (B), high-density lipoprotein cholesterol (HDLC) (C), ALP (D) and AST (E) were determined using Fuji Dri-Chem 7000 V. Data are shown as the mean \pm SE ($n=7$ per group). Differences in means were analyzed by two-way ANOVA with a post hoc test. Overall, a significant main effect was observed in (A), (B), (C), (D) and (E) by diet and (A), (C) and (E) by exposure, with a significant interaction in (E). The T-H group was significantly lower than the V-H group in (A), (C), (D) and (E). Values with different letters indicate a significant difference from each other. See *P*-values in the 'Results'. No statistical comparison was performed between the V-R and T-H groups, or between the T-R and V-H groups.

Glucose Tolerance Test (GTT) and Insulin Resistance Test (IRT)

To study the possible effects of *in utero* and lactational exposure to TCDD on glucose metabolism, we carried out the GTT at weeks 12 and 20 after birth and the IRT at weeks 13 and 21 after birth. The significant main effects of diet were observed in the GTT throughout the test period at week 12 [$F(1,156)=126$, $P<0.001$] and at week 20 [$F(1,156)=183$, $P<0.001$], as shown in Fig. 3A. However, no significant main effect of exposure was found at either of these time points (Fig. 3A).

The significant main effects of diet were also observed in the IRT throughout the test period at week 13 [$F(1,125)=82$, $P<0.001$] and at week 21 [$F(1,130)=181$, $P<0.001$] (Fig. 3B). However, no significant main effect of exposure was observed

(Fig. 3B). The blood glucose concentration in the high-calorie diet groups responded nearly normally to insulin administration, as did the blood glucose concentration in the regular diet groups. This necessitated nullification of our original hypothesis, that *in utero* and lactational exposure to TCDD is involved in the occurrence or aggravation of type 2 diabetes mellitus.

Blood Biochemistry

We examined the blood biochemistry of 15- and 26-week-old mice using two-way ANOVA with the Tukey's HSD post hoc test. At week 15, significant main effects of diet were found on total cholesterol [$F(1,23)=21.6$, $P<0.001$] and HDLC levels [$F(1,23)=16.5$, $P<0.001$], but no significant main effects of diet

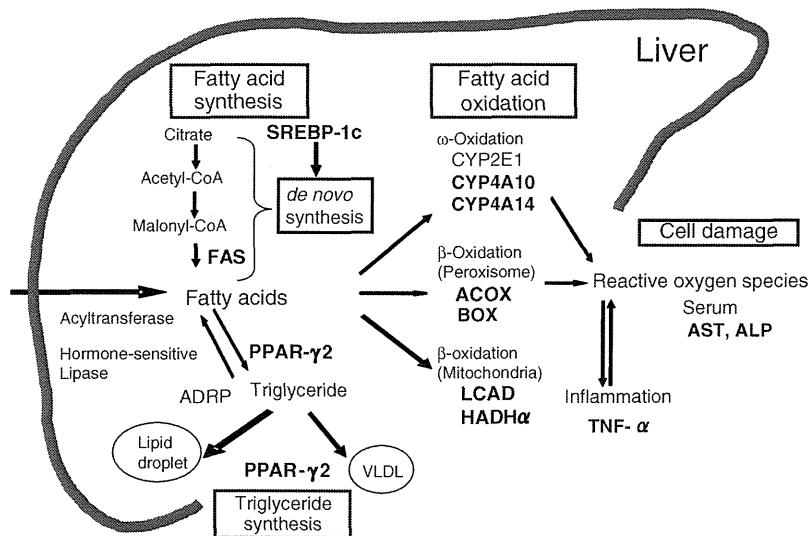


Figure 6. A scheme of fatty acid metabolism in the liver. Genes in the liver and substances in serum analyzed in this study are shown in bold. See abbreviations in text.

or exposure were observed on triglyceride or AST levels (Fig. 4). In contrast, at week 26, comparison of total cholesterol levels yielded significant main effects of exposure [$F(1,26) = 9.78, P < 0.01$] and of diet [$F(1, 26) = 353, P < 0.001$], with a significant difference between the V-H and T-H groups ($P < 0.01$) (Fig. 5A).

A significant main effect of diet was observed on triglyceride levels [$F(1,26) = 5.64, P < 0.05$] (Fig. 5B), but no significant main effect of exposure was observed. By contrast, high-density lipoprotein cholesterol (HDL) levels revealed a significant main effect of both exposure [$F(1,25) = 8.30, P < 0.01$] and

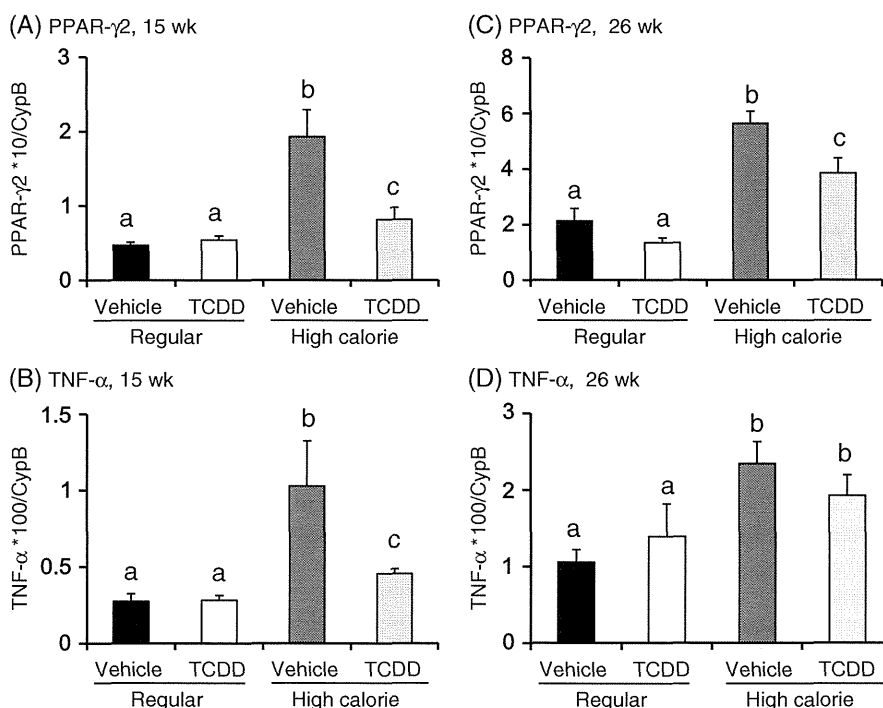


Figure 7. Expression of peroxisomal proliferator-activated receptor PPAR-γ2 (A, C) and tumor necrosis factor TNF-α (B, D) genes in the liver from 15-week old (A, B) and 26-week-old (C, D) mice, exposed to 2,3,7,8-tetrachlorodibenzo-*p*-dioxin (TCDD) *in utero* and via lactation, that were fed a high-calorie diet or a regular diet after weaning. Data are shown as the mean ± SE ($n = 4-5$ per group) after normalization with CypB. Differences in means were analyzed by two-way ANOVA with a post hoc test. Differences in means were analyzed by two-way ANOVA with a post hoc test. Overall, a significant main effect was observed in (A), (B), (C) and (D) by diet, and (A), (B), and (C) by exposure, with a significant interaction in (A) and (C). The T-H group was significantly lower than the V-H group in (A), (B), and (C). Values with different letters indicate a significant difference from each other. See P values in the 'Results'. No statistical comparison was performed between the V-R and T-H groups, or between the T-R and V-H groups.

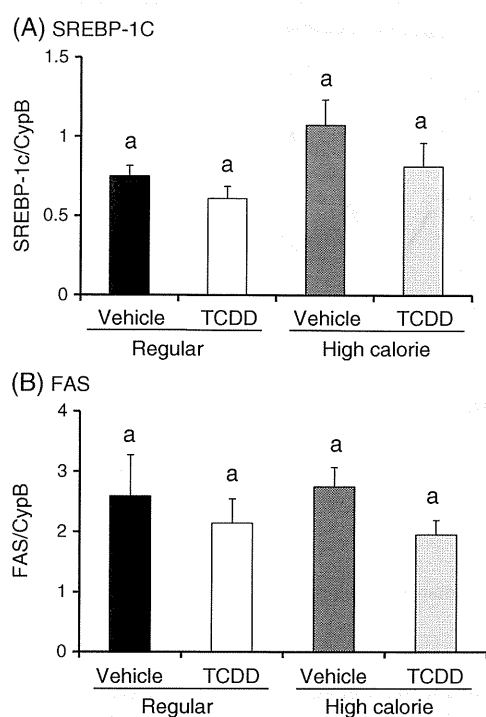


Figure 8. Expressions of SREBP-1c (A) and FAS (B) genes in the liver from 15-week-old mice, exposed to 2,3,7,8-tetrachlorodibenzo-*p*-dioxin (TCDD) *in utero* and via lactation, that were fed a high-calorie diet or a regular diet after weaning. Data are shown as the mean \pm SE ($n=4-5$ per group) after normalization with CypB. Differences in means were analyzed by two-way ANOVA with a post hoc test. Overall, a significant main effect by diet was observed in (A) at $P < 0.05$. No statistical comparison was performed between the V-R and T-H groups, or between the T-R and V-H groups.

of diet [$F(1,25)=432$, $P < 0.001$], again with a significant difference between the V-H and T-H groups ($P < 0.01$) (Fig. 5C). A significant main effect of diet [$F(1,25)=35.7$, $P < 0.001$], but not of exposure, was observed on ALP levels, with a significant difference between the V-H and T-H groups ($P < 0.05$) (Fig. 5d), whereas a significant main effect of exposure [$F(1,25)=5.16$, $P < 0.05$] and of diet [$F(1,25)=45.3$, $P < 0.001$] was observed on AST levels, with a significant interaction between diet and exposure [$F(1,25)=9.77$, $P < 0.01$]. The T-H group was significantly lower than the V-H group ($P < 0.001$) (Fig. 5E).

Lipid Metabolism-related Gene Expression in the Liver

Given our coincidental observation regarding diet-dependent alterations in lipid metabolism, we next investigated how *in utero* and lactational exposure to TCDD affects lipid metabolism-related gene expression (see schematic diagram in Fig. 6). Because the blood biochemistry revealed signs of metabolic syndrome in the high-calorie diet groups at week 15, with marginal signs of liver damage at week 26, we first examined the mRNA expression levels of PPAR- γ 2 and TNF- α in the liver at these time periods.

At week 15, the significant main effects of exposure [$F(1,15)=8.81$, $P < 0.01$] and of diet [$F(1,25)=24.2$, $P < 0.001$] were observed on PPAR- γ 2 mRNA expression levels, with a significant interaction between exposure and diet [$F(1,15)=11.4$,

$P < 0.01$]. The V-H group showed a significantly higher expression level of PPAR- γ 2 mRNA relative to the V-R group, but the enhanced expression of PPAR- γ 2 mRNA was significantly suppressed in the T-H group relative to the V-H group ($P < 0.001$) (Fig. 7A). At week 26, the alterations in mRNA expression levels observed in the liver at week 15 became less marked, but the significant main effects of exposure [$F(1,15)=7.51$, $P < 0.05$] and of diet [$F(1,15)=40.8$, $P < 0.001$] were still found, without a significant interaction between the two factors (Fig. 7C). The increased PPAR- γ 2 mRNA expression levels continued to be significantly suppressed in the T-H group compared with the V-H group ($P < 0.001$) (Fig. 7C). At week 15, the significant main effects of exposure [$F(1,15)=4.95$, $P < 0.05$] and of diet [$F(1,15)=13.5$, $P < 0.01$] were also found on TNF- α mRNA abundance, with a significant interaction between exposure and diet [$F(1,15)=5.28$, $P < 0.05$]. Like PPAR- γ 2 mRNA expression levels, the enhanced TNF- α mRNA expression levels were significantly suppressed in the T-H group versus the V-H group ($P < 0.01$) (Fig. 7B). At week 26, a significant main effect of diet was observed on TNF- α mRNA abundance [$F(1,15)=7.11$, $P < 0.05$], but no significant difference was observed between the V-H and T-H groups (Fig. 7D).

We then focused on the gene expression of lipid metabolism-related genes in the liver at week 15 (see schematic diagram in Fig. 6). First, we examined the mRNA expression levels of SREBP-1c and FAS, both of which are responsible for the *de novo* synthesis of fatty acids in the liver. A significant main effect of diet [$F(1,15)=5.08$, $P < 0.05$], but not of exposure, was found on SREBP-1c mRNA abundance (Fig. 8A), whereas no significant main effect of either exposure or diet was observed on FAS mRNA abundance (Fig. 8B).

Next, we determined the mRNA expression levels for genes that are responsible for the β -oxidation of fatty acids, including LCAD, HADH α , ACOX and BOX (Fig. 9). A significant main effect of diet [$F(1,15)=45.9$, $P < 0.001$], but not of exposure, was observed on LCAD mRNA abundance. The increased LCAD mRNA abundance in the V-H group was significantly attenuated in the T-H group ($P < 0.05$) (Fig. 9A). By contrast, no significant main effect of exposure or of diet was observed on HADH α mRNA abundance (Fig. 9B). A significant main effect of diet [$F(1,15)=22.3$, $P < 0.001$], but not of exposure, was observed on ACOX mRNA levels, and the increased ACOX mRNA levels in the V-H group were significantly suppressed in the T-H group ($P < 0.05$) (Fig. 9C). Finally, BOX mRNA abundance was subject to a significant main effect of diet [$F(1,15)=16.6$, $P < 0.001$], but not of exposure, and the increased BOX mRNA abundance in the V-H group was significantly reduced in the T-H group ($P < 0.05$) (Fig. 9D).

The gene expression levels of CYP4A10 and CYP4A14, which take part in ω -oxidation of fatty acids, were next determined. The significant main effects of exposure [$F(1,14)=4.80$, $P < 0.05$] and of diet [$F(1,25)=31.2$, $P < 0.001$] were found on CYP4A10 mRNA levels. The increased abundance in the V-H group was significantly suppressed in the T-H group ($P < 0.05$) (Fig. 9E). By contrast, a significant main effect of diet only [$F(1,15)=32.1$, $P < 0.001$], was observed on CYP4A14 mRNA levels (Fig. 9F).

Discussion

Epidemiological observations on the association between low birth weight and coronary heart disease later in life, was formulated to be a theory on 'developmental origins of health and

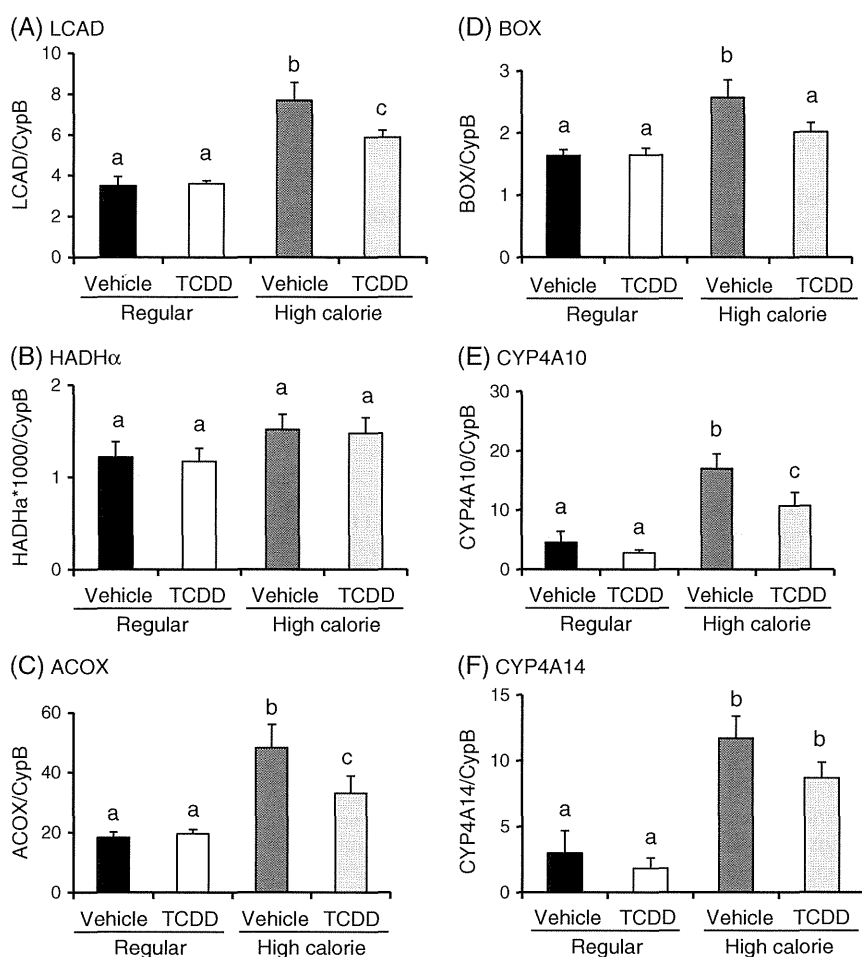


Figure 9. Expressions of long-chain acyl-CoA dehydrogenase (LCAD) (A), HADH α (B), acyl-CoA oxidase (ACOX) (C), branched-chain acyl-CoA oxidase (BOX) (D), CYP4A10 (E), and CYP4A14 (F) in the liver from 15-week-old mice, exposed to 2,3,7,8-tetrachlorodibenzo-*p*-dioxin (TCDD) *in utero* and via lactation, that were fed a high-calorie diet or a regular diet after weaning. Data are shown as the mean \pm SE ($n=4-5$ per group) after normalization with CypB. Differences in means were analyzed by two-way ANOVA with a post-hoc test. No statistical comparison was performed between the V-R and T-H groups, or between the T-R and V-H groups.

disease (DoHAD)' (Barker, 2007). This theory has been supported by a plethora of epidemiological and animal studies, and many environmental factors during gestation, including poor nutritional status and chemical exposure, can be associated with permanent changes in metabolism and chronic disease susceptibility (Bernal and Jirtle, 2010; Newbold *et al.*, 2008; Waterland *et al.*, 2007). Gestational exposure to chemicals, including carcinogens and environmental endocrine disrupting chemicals, has been known to induce altered expression of genes and pathophysiological phenotypes not only later in the life of F1 offspring but also with trans-generational effects (Barouki *et al.*, 2012; Guerrero-Bosagna and Skinner, 2012; Pogribny and Rusyn, 2013), although the latter examples are still limited in number. Based on these lines of evidence, the present study was initiated with the hypothesis in that *in utero* and lactational exposure to TCDD will affect a group of mouse offspring given a high-calorie diet, by aggravating insulin resistance and leading to type 2 diabetes mellitus and hypertension in adulthood. The two groups of mice that received a high-calorie diet for 15 and 26 weeks (vehicle-exposed, V-H, and TCDD-exposed, T-H) were significantly more obese and

had higher blood glucose levels relative to the regular diet groups (V-R and T-R). However, the present result refuted our original hypothesis in that *in utero* and lactational exposure to TCDD aggravates insulin resistance, glucose tolerance, or hypertension.

On the other hand, the group of mice given a high-calorie diet but without prior TCDD exposure (V-H group) had signs of hepatic inflammation, liver damage and altered lipid metabolism (Figs. 5, 7, 8). The present finding is surprising in a way that *in utero* and lactational exposure to TCDD resulted in suppressing effects of lipid dysregulation induced by high-calorie diet in offspring later in adulthood. Although the precise mechanism on the molecular basis remains elusive, epigenetic alterations have been suspected to be responsible for the underlying cause of such phenomena, as has been shown in the examples as described above. In a recent study, adult male Wistar rats given a high-fat diet for 6 weeks were found to have the elevated levels of ethoxyresorufin-*O*-deethylase (EROD) and methoxyresorufin-*O*-demethylase (MROD), the enzymes of which reflect CYP1A1 and 1A2 activities, respectively (Tutelyan *et al.*, 2012). In the present study, the basal expression of CYP1A1

and 1A2 mRNA was reduced by a high-calorie diet. Because the experimental conditions differ between these two studies, the reason for this inconsistency is currently unknown.

TCDD exposure leads to hepatic steatosis in mice (Angrish *et al.*, 2012) and lipid accumulation in the livers of industrial workers (Pelclova *et al.*, 2002). Notably, Lee *et al.* (2010) showed that TCDD-induced hepatic steatosis is mediated in an AhR-dependent manner. In that study, adult mice maintained on a regular diet were given a single oral dose of TCDD (30 $\mu\text{g kg}^{-1}$ body weight). The mice developed hepatic steatosis 1 week after exposure to TCDD. Although the TCDD dose employed in the Lee *et al.* (2010) study was much higher than the dose employed in our study, it is not clear why the direction of TCDD actions on lipid metabolism was reversed. A plausible explanation is that differences in the dosage and timing of TCDD exposure can result in opposing dioxin actions. When the TCDD dose is high and administered to adult animals, altered gene regulation (e.g. CYP1A1 induction), liver toxicity, and signs of lipid metabolism dysregulation (e.g. wasting syndrome) probably occur as a result. However, when the TCDD dose is low and administered to pregnant dams, nearly all of the dioxin is eliminated from the body of the offspring at the time of analysis (Gasiewicz *et al.*, 1983), with no overt signs of toxicity. It is interesting to note that different laboratories have also reported alterations in the higher brain functions of TCDD-exposed rats and mice under such exposure conditions (Markowski *et al.*, 2002; Widholm *et al.*, 2003; Nishijo *et al.*, 2007; Hojo *et al.*, 2008). However, the mechanism of TCDD-induced neurotoxicity remains elusive.

The current study brings forth new questions in terms of why and how *in utero* and lactational exposure to low-dose TCDD can suppress the progression of a fatty liver-related disease state that is provoked by a high-calorie diet. To answer these questions, the administration of multiple doses of TCDD together with the evaluation of the consequences (i.e. pathological/histological outcomes, as well as possible alterations in major parameters of lipid metabolism, such as fatty acid and triglyceride levels in the liver) will be required. Another related question that must be addressed is precisely how *in utero* and lactational exposure to TCDD can dysregulate the expression of genes involved in lipid metabolism later in life.

TCDD reportedly downregulates the mRNA expression levels of PPAR- γ 2, CCAAT enhancer binding protein α (C/EBP α) and lipogenic genes in an AhR-dependent manner during adipocyte differentiation (Alexander *et al.*, 1998; Phillips *et al.*, 1995). Because the elimination half-life of TCDD is approximately 11 days in C57BL/6J mice (Gasiewicz *et al.*, 1983), it is unlikely that gene expression of PPAR- γ 2 in the T-H group was attenuated by an ostensibly negligible amount of TCDD at weeks 15 and 26. This notion is supported by the lack of elevated CYP1A1 and CYP1A2 mRNA levels in the liver in our study. Although the underlying mechanism is still unclear, the present results suggest that *in utero* and lactational exposure to TCDD modulates the epigenetic state of PPAR- γ 2 and related transcription factors. Furthermore, such exposure to TCDD may suppress the elevated expression of PPAR- γ 2 later in adulthood that is responsible for enhanced lipid accumulation into hepatocytes, as well as the selective upregulation of adipogenic and lipogenic gene expression (Schadinger *et al.*, 2005).

In conclusion, mice fed a high-calorie diet developed dysregulation of lipid metabolism and marginal signs of liver inflammation and liver damage, but exposure to low-dose TCDD

in utero and during lactation lessened such effects by an as yet unidentified mechanism. The present animal model may therefore prove useful for future studies aimed at the elucidation of the molecular mechanisms behind TCDD modulation of molecular programming during fetal development.

Acknowledgments

This study was supported in part by a research grant from the Ministry of the Environment (to C.T.). The authors thank Mr M. Takahashi and Mr T. Higashide (Sankyo Lab Service Co., Tokyo) for their excellent assistance in the maintenance of animals.

References

- Alexander DL, Ganem LG, Fernandez-Salguero P, Gonzalez F, Jefcoate CR. 1998. Aryl-hydrocarbon receptor is an inhibitory regulator of lipid synthesis and of commitment to adipogenesis. *J. Cell Sci.* **111**(Pt 22): 3311–3322.
- Angrish MM, Mets BD, Jones AD, Zacharewski TR. 2012. Dietary fat is a lipid source in 2,3,7,8-tetrachlorodibenzo-p-dioxin (tcdd)-elicited hepatic steatosis in C57BL/6 Mice. *Toxicol. Sci.* **128**: 377–386.
- Barker DJ. 2007. The origins of the developmental origins theory. *J. Intern. Med.* **261**: 412–417.
- Barouki R, Gluckman PD, Grandjean P, Hanson M, Heindel JJ. 2012. Developmental origins of non-communicable disease: implications for research and public health. *Environ. Health.* **11**:42. doi: 10.1186/1476-069X-11-42. (Open access online journal)
- Bernal AJ, Jirtle RL. 2010. Epigenomic disruption: the effects of early developmental exposures. *Birth Defects Res. A Clin. Mol. Teratol.* **88**: 938–944.
- Cranmer M, Louie S, Kennedy RH, Kern PA, Fonseca VA. 2000. Exposure to 2,3,7,8-tetrachlorodibenzo-p-dioxin (TCDD) is associated with hyperinsulinemia and insulin resistance. *Toxicol. Sci.* **56**: 431–436.
- Everett CJ, Frithsen IL, Diaz VA, Koopman RJ, Simpson WM Jr, Mainous AG, 3rd. 2007. Association of a polychlorinated dibenzo-p-dioxin, a polychlorinated biphenyl, and DDT with diabetes in the 1999-2002 National Health and Nutrition Examination Survey. *Environ. Res.* **103**: 413–418.
- Fierens S, Mairesse H, Heilier JF, De Burbure C, Focant JF, Eppe G, De Pauw E, Bernard A. 2003. Dioxin/polychlorinated biphenyl body burden, diabetes and endometriosis: findings in a population-based study in Belgium. *Biomarkers* **8**: 529–534.
- Fujiyoshi PT, Michalek JE, Matsumura F. 2006. Molecular epidemiologic evidence for diabetogenic effects of dioxin exposure in U.S. Air force veterans of the Vietnam war. *Environ. Health Perspect.* **114**: 1677–1683.
- Gasiewicz TA, Geiger LE, Rucci G, Neal RA. 1983. Distribution, excretion, and metabolism of 2,3,7,8-tetrachlorodibenzo-p-dioxin in C57BL/6J, DBA/2J, and B6D2F1/J mice. *Drug Metab. Dispos.* **11**: 397–403.
- Guerrero-Bosagna C, Skinner MK. 2012. Environmentally induced epigenetic transgenerational inheritance of phenotype and disease. *Mol. Cell. Endocrinol.* **354**: 3–8.
- Hojo R, Kakeyama M, Kurokawa Y, Aoki Y, Yonemoto J, Tohyama C. 2008. Learning behavior in rat offspring after *in utero* and lactational exposure to either TCDD or PCB126. *Environ. Health Prev. Med.* **13**: 169–180.
- La Merrill M, Harper R, Birnbaum LS, Cardiff RD, Threadgill DW. 2010. Maternal dioxin exposure combined with a diet high in fat increases mammary cancer incidence in mice. *Environ. Health Perspect.* **118**: 596–601.
- Lee JH, Wada T, Febbraio M, He J, Matsubara T, Lee MJ, Gonzalez FJ, Xie W. 2010. A novel role for the dioxin receptor in fatty acid metabolism and hepatic steatosis. *Gastroenterology* **139**: 653–663.
- Li X, Weber LWD, Rozman KK. 1995. Toxicokinetics of 2,3,7,8-tetrachlorodibenzo-p-dioxin in female Sprague-Dawley rats including placental and lactational transfer to fetuses and neonates. *Fundam. Appl. Toxicol.* **27**: 70–76.
- Malassiné A, Frendo JL, Evain-Brion D. 2003. A comparison of placental development and endocrine functions between the human and mouse model. *Hum. Reprod. Update* **9**: 531–539.

- Markowski VP, Cox C, Preston R, Weiss B. 2002. Impaired cued delayed alternation behavior in adult rat offspring following exposure to 2,3,7,8-tetrachlorodibenzo-*p*-dioxin on gestation day 15. *Neurotoxicol. Teratol.* **24**: 209–218.
- Michalek JE, Akhtar FZ, Kiel JL. 1999. Serum dioxin, insulin, fasting glucose, and sex hormone-binding globulin in veterans of Operation Ranch Hand. *J. Clin. Endocrinol. Metab.* **84**: 1540–1543.
- Newbold RR, Padilla-Banks E, Jefferson WN, Heindel JJ. 2008. Effects of endocrine disruptors on obesity. *Int. J. Androl.* **31**: 201–208.
- Nishijo M, Kuriwaki J, Hori E, Tawara K, Nakagawa H, Nishijo H. 2007. Effects of maternal exposure to 2,3,7,8-tetrachlorodibenzo-*p*-dioxin on fetal brain growth and motor and behavioral development in offspring rats. *Toxicol. Lett.* **173**: 41–47.
- Nishimura N, Yonemoto J, Nishimura H, Ikushiro S, Tohyama C. 2005. Disruption of thyroid hormone homeostasis at weaning of Holtzman rats by lactational but not in utero exposure to 2,3,7,8-tetrachlorodibenzo-*p*-dioxin. *Toxicol. Sci.* **85**: 607–614.
- Ogawa R, Mizuno H, Watanabe A, Migita M, Hyakusoku H, Shimada T. 2004. Adipogenic differentiation by adipose-derived stem cells harvested from GFP transgenic mice-including relationship of sex differences. *Biochem. Biophys. Res. Commun.* **319**: 511–517.
- Pelclova D, Fenclova Z, Preiss J, Prochazka B, Spacil J, Dubska Z, Okrouhlik B, Lukas E, Urban P. 2002. Lipid metabolism and neuropsychological follow-up study of workers exposed to 2,3,7,8-tetrachlorodibenzo-*p*-dioxin. *Int. Arch. Occup. Environ. Health* **75**(Suppl): S60–66.
- Phillips M, Enan E, Liu PC, Matsumura F. 1995. Inhibition of 3T3-L1 adipose differentiation by 2,3,7,8-tetrachlorodibenzo-*p*-dioxin. *J. Cell Sci.* **108**(Pt 1): 395–402.
- Pogribny IP, Rusyn I. 2013. Environmental toxicants, epigenetics, and cancer. *Adv. Exp. Med. Biol.* **754**: 215–232.
- Pohjanvirta R, Tuomisto J. 1994. Short-term toxicity of 2,3,7,8-tetrachlorodibenzo-*p*-dioxin in laboratory animals: effects, mechanisms, and animal models. *Pharmacol. Rev.* **46**: 483–549.
- Sato S, Shirakawa H, Tomita S, Ohsaki Y, Haketa K, Tooi O, Santo N, Tohkin M, Furukawa Y, Gonzalez FJ, Komai M. 2008. Low-dose dioxins alter gene expression related to cholesterol biosynthesis, lipogenesis, and glucose metabolism through the aryl hydrocarbon receptor-mediated pathway in mouse liver. *Toxicol. Appl. Pharmacol.* **229**: 10–19.
- Schadinger SE, Bucher NL, Schreiber BM, Farmer SR. 2005. PPARgamma2 regulates lipogenesis and lipid accumulation in steatotic hepatocytes. *Am. J. Physiol. Endocrinol. Metab.* **288**: E1195–1205.
- Terauchi Y, Iwamoto K, Tamemoto H, Komeda K, Ishii C, Kanazawa Y, Asanuma N, Aizawa T, Akanuma Y, Yasuda K, Kodama T, Tobe K, Yazaki Y, Kadowaki T. 1997. Development of non-insulin-dependent diabetes mellitus in the double knockout mice with disruption of insulin receptor substrate-1 and beta cell glucokinase genes. Genetic reconstitution of diabetes as a polygenic disease. *J. Clin. Invest.* **99**: 861–866.
- Tutelyan VA, Trusov NV, Guseva GV, Beketova NA, Aksenov IV, Kravchenko LV. 2012. Indole-3-carbinol induction of CYP1A1, CYP1A2, and CYP3A1 activity and gene expression in rat liver under conditions of different fat content in the diet. *Bull. Exp. Biol. Med.* **154**: 250–254.
- Van den Berg M, Birnbaum LS, Denison M, De Vito M, Farland W, Feeley M, Fiedler H, Hakansson H, Hanberg A, Haws L, Rose M, Safe S, Schrenk D, Tohyama C, Tritscher A, Tuomisto J, Tysklind M, Walker N, Peterson RE. 2006. The 2005 World Health Organization reevaluation of human and Mammalian toxic equivalency factors for dioxins and dioxin-like compounds. *Toxicol. Sci.* **93**: 223–241.
- Vena J, Boffetta P, Becher H, Benn T, Bueno-de-Mesquita HB, Coggon D, Colin D, Flesch-Janys D, Green L, Kauppinen T, Littorin M, Lyngge E, Mathews JD, Neuberger M, Pearce N, Pesatori AC, Saracci R, Steenland K, Kogevinas M. 1998. Exposure to dioxin and nonneoplastic mortality in the expanded IARC international cohort study of phenoxy herbicide and chlorophenol production workers and sprayers. *Environ. Health Perspect.* **106**(Suppl 2): 645–653.
- Waterland RA, Travisano M, Tahiliani KG. 2007. Diet-induced hypermethylation at agouti viable yellow is not inherited transgenerationally through the female. *FASEB J.* **21**: 3380–5.
- Widholm JJ, Seo BW, Strupp BJ, Seegal RF, Schantz SL. 2003. Effects of perinatal exposure to 2,3,7,8-tetrachlorodibenzo-*p*-dioxin on spatial and visual reversal learning in rats. *Neurotoxicol. Teratol.* **25**: 459–71.



Prenatal zinc deficiency-dependent epigenetic alterations of mouse metallothionein-2 gene[☆]

Hisaka Kurita^a, Seiichiroh Ohsako^a, Shin-ichi Hashimoto^b, Jun Yoshinaga^c, Chiharu Tohyama^{a,*}

^aLaboratory of Environmental Health Sciences, Center for Disease Biology and Integrative Medicine, Graduate School of Medicine, The University of Tokyo, 7-3-1 Hongo, Bunkyo-ku, Tokyo 113-0033, Japan

^bDepartment of Molecular Preventive Medicine, Graduate School of Medicine, The University of Tokyo, Hongo, Bunkyo-ku, Tokyo, Japan

^cDepartment of Environmental Studies, The University of Tokyo, Kashiwanoha, Kashiwa, Chiba, Japan

Received 14 February 2012; received in revised form 29 April 2012; accepted 7 May 2012

Abstract

Zinc (Zn) deficiency *in utero* has been shown to cause a variety of disease states in children in developing countries, which prompted us to formulate the hypothesis that fetal epigenetic alterations are induced by zinc deficiency *in utero*. Focusing on metallothionein (MT), a protein that contributes to Zn transport and homeostasis, we studied whether and how the prenatal Zn status affects gene expression. Pregnant mice were fed low-Zn (IU-LZ, 5.0 µg Zn/g) or control (IU-CZ, 35 µg Zn/g) diet *ad libitum* from gestation day 8 until delivery, with a regular diet thereafter. Bisulfite genomic sequencing for DNA methylation and chromatin immunoprecipitation assay for histone modifications were performed on the *MT2* promoter region. We found that 5-week-old IU-LZ mice administered cadmium (Cd) (5.0 mg/kg b.w.) have an elevated abundance of *MT2* mRNA compared with IU-CZ mice. Alteration of histone modifications in the *MT2* promoter region having metal responsive elements (MREs) was observed in 1-day-old and 5-week-old IU-LZ mice compared with IU-CZ mice. In addition, prolongation of MTF1 binding to the *MT2* promoter region in 5-week-old IU-LZ mice upon Cd exposure is considered to contribute to the enhanced *MT2* induction. In conclusion, we found for the first time that Zn deficiency *in utero* induces fetal epigenetic alterations and that these changes are being stored as an epigenetic memory until adulthood.

© 2013 Elsevier Inc. All rights reserved.

Keywords: DNA methylation; Epigenetics; Histone modification; Metallothionein; Zinc

1. Introduction

The malnutritional status *in utero* has been shown to affect the progeny's health and disease states later in life in humans as well as in laboratory animals. Low-birth-weight babies resulted from prenatal malnutrition can be a risk factor for lifestyle-related diseases, such as ischemic heart disease and diabetes [1–4]. This hypothesis has been widely acknowledged and expanded to the concept, named 'Developmental origins of health and disease (DOHaD)' [5]. Recently, rats that were grown under low-protein nutritional conditions *in utero*, or had intrauterine growth retardation have been shown to develop hypertension or type 2 diabetes later in adulthood [6–9]. Moreover, a plethora of published works have shown that extrinsic conditions *in utero*, such as nutrition and environmental chemicals, affect the propensity of the fetus to develop disease states later in adulthood

[10–12]. Although the underlying mechanism is still under intensive investigation, there is a widely-acknowledged view that epigenetic alterations, namely, DNA methylation (the covalent addition of a methyl group to the 5'-carbon of cytosine in the CpG dinucleotide) and histone modification (methylation, acetylation, phosphorylation, ADP-ribosylation, and ubiquitination), play a pivotal role in the expression of particular genes, which will subsequently alter the physiological status of the whole organism. Gene expression is suppressed by DNA methylation of the promoter region of a given gene [13], whereas histone modifications regulate chromatin structure and alter gene activity [14]. Such epigenetic alterations could be inherited by succeeding generations [15].

Experimentally, a few studies have shown that zinc (Zn) restriction during pregnancy induces disease states later in life. Rats grown under prenatal or postnatal Zn restriction have been reported to develop hypertension [16] and impairments of learning and memory [17,18] later in adulthood. Pregnant mice fed a Zn-deficient diet *in utero* have shown persistent immunodeficiency for three succeeding generations [19]. Zn is an essential trace element and a key component of approximately 300 enzymes in various types of tissues [20,21]. Zn deficiency induces various disease states in humans, such as immunodeficiency, developmental disorders, alopecia, dysgeusia, skin disorders and anemia. Vegetarians [22], elderly

[☆] Grants and Funding Sources: This study was supported by a Grant-in-Aid for Challenging Exploratory Research (21651022) from the Japan Society for Promotion of Science (JSPS) (to CT) and Research Fellowships for Young Scientists (224083) from JSPS and Global COE Program "Medical System Innovation on Multidisciplinary Integration" from MEXT, Japan (to HK).

* Corresponding author. Tel.: +81 3 5841 1431; fax: +81 3 5841 1434.

E-mail address: mtohyama@mail.ecc.u-tokyo.ac.jp (C. Tohyama).

persons [23], habitual alcohol drinkers [24], infants and pregnant/parturient women [22] have the tendency to develop Zn deficiency. In addition, maternal Zn deficiency during pregnancy induces pregnancy complications, delayed delivery, and low-body-weight birth [25]. Zn deficiency is responsible for 4.4% of deaths of children aged 6–59 months in developing countries [26].

Metallothionein (MT), a low-molecular weight protein, has been shown to be involved in the transport, metabolism and homeostasis of heavy metal ions, such as Zn and copper, in tissues and cells. One-third of their amino acid residues of this protein are cysteine residues without a disulfide bond. This characteristic enables MTs to play a role in the transport and inactivation/detoxification of metals [27,28]. Aside from the metabolism and homeostasis of heavy metals, MT has been known to protect cells from oxidative stress and inflammation elicited by various environmental stimuli including heavy metals. Among the four MT isoforms known so far, MT1 and MT2 exist in nearly all types of cells in the body. It has been established that the expression of *MT1/2* genes is induced by metal ions, such as Cd, Zn, Cu and Hg [27]. For the up-regulation of *MT1/2* transcription upon exposure to these metal ions, metal responsive elements (MREs) located in the promoter region are essential. A limited line of experimental evidence showed that metal transcription factor 1 (MTF1) [29] will bind to the MRE motif upon exposure to at least Zn ions, and the Zn-ion-bound MTF1 forms a complex with p300 and Sp1, and then this complex is recruited to MREs of the *MT1* promoter region [30].

The effects of prenatal zinc deficiency on MT regulation have been studied. Pregnant mice were fed either a control diet (100 µg Zn/g) or a low-Zn diet (5.0 µg Zn/g) from gestation day 7 to delivery, and both groups of dams were given the control diet after delivery. Although the Zn and MT levels in pups born to these two groups of dams were similar at postnatal day 3, serum IgM concentrations were significantly lower in adulthood in the mouse offspring born to dams given the low-Zn diet than in the offspring born to control dams. Moreover, when the mouse offspring was given Zn injections to stimulate MT synthesis, the mice deprived of Zn while *in utero* had markedly higher MT levels in the liver than control mice later in adulthood [31].

Collectively, prenatal Zn deficiency has been shown to induce disease states, which is presumably due to epigenetic alterations. However, nearly no studies to elucidate the molecular basis of disease states induced by prenatal Zn deficiency are available. Thus, we have hypothesized that fetal epigenetic alterations can be induced by Zn deficiency *in utero* and alter the physiological conditions that will lead to the onset of disease conditions later in adulthood. In this study, we developed an experimental animal model of prenatal Zn deficiency and studied whether Zn deficiency *in utero* exerts fetal epigenetic alterations in *MT1/2* genes.

2. Materials and methods

2.1. Reagents

The following reagents were purchased from the manufacturers described in parentheses: RNase A, mouse monoclonal anti-β-actin IgG1 and CellLyticNuCLEARExtraction kit (Sigma-Aldrich, St Louis, MO, USA); RNeasy Mini kit, QIAquick PCR Purification kit, QIAquick Gel Extraction kit and QIAprep Spin Miniprep kit (Qiagen K.K., Tokyo, Japan); Lipofectamine 2000 (Invitrogen, Carlsbad, CA, USA); Wizard DNA Clean-Up system, pGEM-T Easy Vector, pGL4.0 Luciferase Reporter Vector, pRL-TK Vector and Dual-Luciferase Reporter Assay System (Promega, Madison, WI, USA); proteinA agarose/salmon sperm DNA, rabbit polyclonal anti-acetylated histone H3 IgG, rabbit polyclonal anti-acetylated histone H4 IgG, rabbit polyclonal anti-acetylated histone H3 lysine14 IgG and Immobilon-P transfer membrane (MilliPore, Billerica, MA, USA); proteinase K, Blocking One and Chemi-Lumi One (Nacalai Tesque, Kyoto, Japan, USA). *Bam* HI, *Aci* I, *Kpn* I, *Xho* I and *Dpn* I were purchased from New England Biolabs Japan (Tokyo, Japan); rabbit polyclonal anti-MTF1 IgG and goat polyclonal anti-lamin B (Santa Cruz Biotechnology, Santa Cruz, CA, USA); Big Dye Terminator v3.1 Cycle Sequencing kit (Applied Biosystems, Foster City, CA, USA); Immunopure goat anti-rabbit IgG, F(ab')₂, peroxidase conjugated, ImmunoPure goat anti-mouse IgG, F(ab')₂, peroxidase conjugated and Immuno Pure rabbit anti-goat IgG, F(ab')₂, peroxidase

conjugated (Thermo Fisher Scientific, Rockford, IL, USA); rabbit polyclonal anti-acetylated histone H3 lysine9 IgG and rabbit polyclonal anti-trimethylated histone H3 lysine4 IgG (Cell Signaling Technology, Danvers, MA, USA); LightCycler480 SYBR Green I Master (Roche Diagnostics Japan, Tokyo, Japan); Minisart SRP 15 (Sartorius Stedim Biotech, Goettingen, Germany); IGEPAL-CA630 (Wako Pure Chemical, Osaka, Japan); PrimeScript RT reagent kit, SYBR Premix Ex Taq, TaKaRa Ex Taq, LA Taq and T4 polynucleotide kinase (TaKaRa BIO, Otsu, Japan). *Nor* I, DH5α and KOD -Plus (Toyobo, Osaka, Japan); Ligation Convenience kit and ISOGEN (Nippon Gene, Tokyo, Japan); all other reagents of analytical grade (Sigma-Aldrich, Invitrogen and Wako Pure Chemical); all oligonucleotides (Hokkaido System Science, Sapporo, Japan).

2.2. Animals

C57BL/6J strain pregnant ($n=44$) and male mice ($n=18$) were purchased from CLEA Japan. The mice were housed in a room with temperature at $23\pm 1^\circ\text{C}$ and humidity at $50\pm 10\%$ on a 12/12-h light–dark cycle. We used three kinds of rodent chow. Laboratory rodent chow (50 µg Zn/g; Labo MR Stock, Nosan) was given to mice unless specifically described. Low-Zn diet (5.0 µg Zn/g) or control diet (35 µg Zn/g) (CLEA Japan) was used in Zn-deficiency experiments. According to the previous studies [32,33], zinc concentration in diet (35 µg Zn/g) was found to be high enough to be used for a control diet group. These chows and deionized water were provided *ad libitum*. For this study, male mice were used unless specifically described. The experiments protocols using mice were approved by the Animal Care and Use Committee of the Graduate School of Medicine, the University of Tokyo.

2.3. Experiments on Zn deficiency *in utero*

Pregnant mice were fed a Labo MR Stock rodent chow until gestation day 7, and the chow was replaced with a low-Zn diet or a control diet thereafter until delivery. On the day of birth, two to three male pups per dam were randomly adopted from fourteen dams to minimize possible litter effects and to make two groups: (1) *in utero* low-Zn (IU-LZ) mice and (2) *in utero* control (IU-CZ) mice. The pups were decapitated by scissors, and their livers were harvested. All the liver tissues except those used for chromatin immunoprecipitation (ChIP) assay were immediately frozen in liquid nitrogen, and kept at -80°C until analyses. Livers used for the ChIP assay were immediately minced by scissors and subjected to the subsequent processes as described in the ChIP assay section below. The number of pups for each dam was adjusted to be 6 to 7 pups by adoption from other dams on the day of birth. The dams were given Labo MR Stock rodent chow from the delivery to weaning. After weaning, male pups were given Labo MR Stock rodent chow thereafter.

When IU-CZ mice and IU-LZ mice became 5 weeks old, they were administered orally with a single dose of cadmium (Cd) (5.0 mg kg^{-1} b.w.). Mice were sacrificed by cervical dislocation, and livers were harvested 0, 1 and 6 h post Cd administration (Fig. 1A).

2.4. Experiment on Zn deficiency in adulthood

Male mice aged 10 weeks were fed a low-Zn (AD-LZ) diet or a control (AD-CZ) diet *ad libitum* for 12 days, and then sacrificed by cervical dislocation to harvest the liver. Other mice were fed Labo MR Stock rodent chow for another 30 days, and administered orally a single dose of Cd (5.0 mg kg^{-1} b.w.). Livers were collected 6 h after Cd administration (Fig. 1B).

2.5. Measurement of Zn and Cd concentrations

Livers (approx. 0.1 g) and blood (approx. 0.2 g) specimens were digested in 2 ml of concentrated nitric acid in glass test tubes. The temperatures were kept at 80°C for 1 h, with a gradual increase with 10°C for 1 h each to 130°C . When the acid-digested specimens were became transparent, they were diluted with 1% HNO_3 and filtered with Minisart SRP 15 and determined for Zn and Cd concentrations by inductively coupled plasma mass spectrometer (Agilent 7500ce; Agilent Technologies).

2.6. RNA isolation and reverse transcription

Total RNA was isolated using RNeasy Mini Kit and then reverse-transcribed using PrimeScript RT reagent Kit, according to the manufacturer's instructions.

2.7. DNA isolation

DNA was isolated using ISOGEN, according to the manufacturer's instructions and purified by phenol/chloroform extraction method.

2.8. Quantitative polymerase chain reaction

Quantitative polymerase chain reaction (qPCR) analysis was performed using SYBR Premix Ex Taq and amplified by LightCycler under the following conditions: $95^\circ\text{C}/10\text{ s} \times 1$ cycle; $95^\circ\text{C}/5\text{ s}$, $60^\circ\text{C}/30\text{ s}$, $\times 45$ cycles or using LightCycler480 SYBR Green I Master and amplified by LightCycler480 under the following conditions: $95^\circ\text{C}/5\text{ min} \times 1$ cycle; $95^\circ\text{C}/15\text{ s}$, $60^\circ\text{C}/10\text{ s}$, $72^\circ\text{C}/30\text{ s} \times 45$ cycles. Primers used in the qPCR analysis

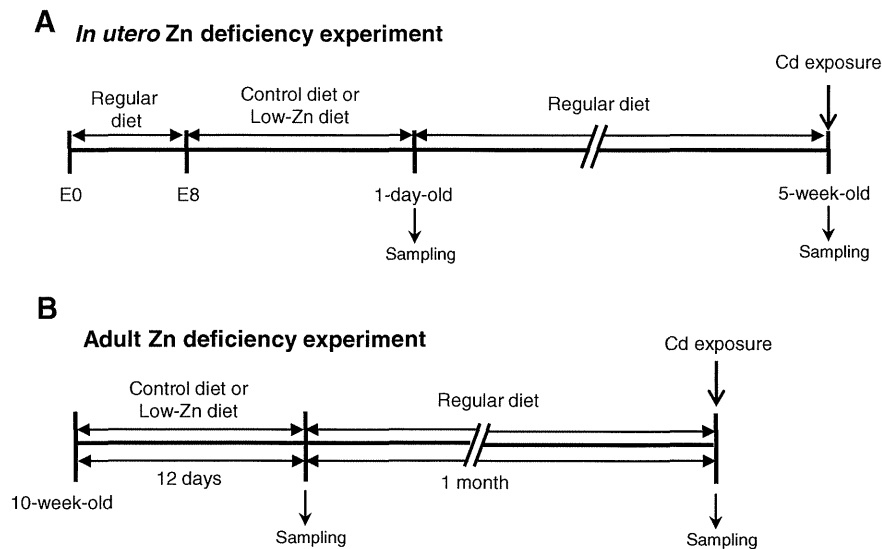


Fig. 1. Study design. (A) Pregnant mice were fed a regular diet until Gestation Day 7, and the chow was replaced with a low-Zn diet or control diet thereafter until delivery. On the day of birth, male pups were divided into two groups: (1) *in utero* low-Zn (IU-LZ) mice and (2) *in utero* control-Zn (IU-CZ) mice. Livers were harvested from a group of 1-day-old male pups. The dams were given Labo MR Stock rodent chow from the delivery to weaning. After weaning, male pups were given Labo MR Stock rodent chow thereafter. When IU-CZ mice and IU-LZ mice became 5 weeks old, they were administered orally a single dose of Cd ($5.0 \text{ mg kg}^{-1} \text{ b.w.}$) and sacrificed by cervical dislocation, and livers were collected 0, 1 and 6 h after Cd administration. (B) Male mice aged 10 weeks were fed a low-Zn diet (AD-LZ) or control diet (AD-CZ) ad libitum for 12 days and then sacrificed by cervical dislocation, and livers were collected. Other mice were fed a regular diet for another 30 days and administered orally a single dose of Cd ($5.0 \text{ mg kg}^{-1} \text{ b.w.}$). Livers were collected 6 h after Cd administration.

are described in Table S1. All primer sets were designed by using Primer3 [34]. All quantitative data were calculated by dividing the copy number of targets by the original RNA concentration, according to a previous study [35].

2.9. Bisulfite genomic sequencing

Mouse genomic DNA was digested with *Not I* and bisulfite conversion reaction was performed as previously described [36]. The bisulfite-treated DNA was cleaned up using Wizard DNA Clean-Up system and amplified by nested PCR method using Ex Taq under the following conditions for the first and second PCRs: $94^\circ\text{C}/2 \text{ min} \times 1 \text{ cycle}$; $94^\circ\text{C}/2 \text{ min}$, $50^\circ\text{C}/2 \text{ min}$, $72^\circ\text{C}/3 \text{ min}$, $\times 5 \text{ cycles}$; $94^\circ\text{C}/2 \text{ min}$, $50^\circ\text{C}/2 \text{ min}$, $72^\circ\text{C}/30 \text{ s}$, $\times 5 \text{ cycles}$; $72^\circ\text{C}/5 \text{ min} \times 25 \text{ cycles}$. Each primer set for the nested amplification is shown in Table S2. All primers were designed using Methyl Primer Express Software v1.0 (Applied Biosystems). The amplified DNA was purified using QIA quick PCR Purification kit and ligated into pGEM-T Easy Vector and transformed into DH5 α . Colony PCR was performed to amplify target DNAs using Ex Taq and M13 primers. The PCR products were sequenced using Big Dye Terminator v3.1 Cycle Sequencing kit and analyzed using 3730 DNA Analyzer (Applied Biosystems).

2.10. Methylation frequency analysis

Purified DNA was digested with *Bam HI*. The digested DNA solution was divided into two portions. One portion was digested with the methylation-sensitive *Aci I*, whereas the other was kept as it was. These *Aci I*-digested and non-digested DNA was subjected to qPCR using SYBR Premix Ex Taq and amplified by LightCycler under the following conditions: $95^\circ\text{C}/10 \text{ s} \times 1 \text{ cycle}$; $95^\circ\text{C}/5 \text{ s}$, $60^\circ\text{C}/15 \text{ s}$, $72^\circ\text{C}/20 \text{ s}$, $\times 40 \text{ cycles}$. Ch-R1 primer sets described in Table S3. The DNA methylation frequency was represented as copy numbers of *Aci I*-digested DNA/copy numbers of non-digested DNA.

2.11. Chromatin Immunoprecipitation assay

The ChIP assay was performed by the essentially same method as previously described [37], with some modifications: the minced mouse liver was cross-linked with 1% formaldehyde for 10 min at room temperature, followed by addition of glycine to be a final concentration of 125 mM and by incubation for 5 min. The cross-linked liver specimen was homogenized using a Dounce homogenizer (catalog# 432–1273, Wheaton) and washed with phosphate-buffered saline three times. The pellet was dissolved in lysis buffer (5.0 mM Tris-HCl, pH 8.1, containing 1.0% sodium dodecyl sulfate [SDS], 10 mM EDTA). It was subjected to sonication by Bioruptor UCD-250HSA (Cosmo Bio) to make an average chromatin fragment size to be 200 to 1000 bp. ProteinA agarose and salmon sperm DNA were added to the fragmented DNA solution, and it was incubated for 1 h at 4°C to eliminate nonspecific substances. An aliquot of the sample was diluted by adding dilution buffer (16.6 mM Tris-HCl, pH 8.1, containing 0.01% SDS, 1.1% Triton X-100, 1.2 mM EDTA, and 167 mM NaCl) and incubated with an

antibody at 4°C overnight. The sample was immunoprecipitated with ProteinA agarose and salmon sperm DNA and washed consecutively with the following four kinds of buffers: low-salt immune complex buffer (20 mM Tris-HCl, pH 8.1, containing 0.1% SDS, 1.0% Triton X-100, 2.0 mM EDTA, and 0.15 M NaCl), high-salt immune complex buffer (20 mM Tris-HCl, pH 8.1, containing 0.1% SDS, 1.0% Triton X-100, 2.0 mM EDTA, and 0.5 M NaCl), LiCl immune complex buffer (10 mM Tris-HCl, pH 8.1, containing 1.0% IGEPAL-CA630, 1.0 mM EDTA, 0.25 M LiCl, 1.0% deoxycholic acid), and TE buffer. The immunoprecipitated DNA was eluted with buffer (0.1 M NaHCO $_3$, pH 8.5, containing 1.0% SDS and 10 mM DTT). Cross-link was removed by an addition of 5.0 M NaCl with incubation at 65°C overnight. The resultant DNA was treated with RNase A for 30 min and proteinase K for 1 h, and the DNA was purified by using QIA quick PCR Purification kit. Quantitative real time PCR was carried out with the DNA using SYBR Premix Ex Taq and amplified by LightCycler under the following conditions: $95^\circ\text{C}/10 \text{ s} \times 1 \text{ cycle}$; $95^\circ\text{C}/5 \text{ s}$, $60^\circ\text{C}/15 \text{ s}$, $72^\circ\text{C}/20 \text{ s}$, $\times 60 \text{ cycles}$ or using LightCycler480 SYBR Green I Master and amplified by LightCycler480 under the following conditions: $95^\circ\text{C}/5 \text{ min} \times 1 \text{ cycle}$; $95^\circ\text{C}/15 \text{ s}$, $60^\circ\text{C}/10 \text{ s}$, $72^\circ\text{C}/30 \text{ s} \times 65 \text{ cycles}$. Primers used in this assay are described in Table S3.

2.12. Western blotting

Nuclear and cytosolic proteins were extracted from mouse liver using CellLyticNucLEARExtraction kit according to the manufacturer's instructions. The protein specimens (25 μg protein/lane) were separated on a 10% SDS-polyacrylamide gel and blotted on an Immobilon-P transfer membrane. The blotted membrane was blocked with Blocking One at room temperature for 1 h. Primary antibody was applied at 4°C overnight, with a dilution factor as described in parentheses: anti-MTF IgG (1:10,000), β -actin IgG1 (1:4,000) and anti-laminB IgG (1:1,000). The 5,000-fold diluted secondary antibody was applied at room temperature for 1 h. The antigen-antibody complexes were visualized by using Chemi-Lumi One. For quantitative analysis, the chemiluminescence intensity of respective bands was quantified using CS analyzer ver.2.02b (ATTO).

2.13. Plasmid constructs

The DNA fragment containing *Kpn I* and *Xho I* restriction sites of $-2,166$ to -17 in the *MT2* promoter was amplified from mouse hepatic DNA by PCR method using LA Taq under the following conditions: $95^\circ\text{C}/1 \text{ min} \times 1 \text{ cycle}$; $95^\circ\text{C}/30 \text{ s}$, $60^\circ\text{C}/1 \text{ min}$, $72^\circ\text{C}/2 \text{ min}$, $\times 30 \text{ cycles}$; $72^\circ\text{C}/10 \text{ min} \times 1 \text{ cycle}$. Primers used for the qPCR are described in Table S4. This fragment was inserted into pGEM-T Easy Vector using Ligation Convenience kit. This plasmid was transformed to DH5 α and cloned. The cloned plasmid was digested by *Kpn I* and *Xho I*. The inserted fragment was separated by electrophoresis in agarose gel and purified by QIAquickGel extraction kit. This purified fragment was inserted into pGL4.0 Luciferase Reporter Vector digested by *Kpn I* and *Xho I*. This construct was named as *pGL4MT2-2166*. The *MT2* MRE-deletion constructs

(Fig. 4B) were made from *pGL4MT2 -2166* as a template by inverse PCR method as follows. The MRE-deletion fragments were amplified from *pGL4MT2-2166* construct by PCR method using KOD-Plus under the following conditions: 94°C/2 min × 1 cycle; 98°C/10 s, 68°C/2 min, × 10 cycles. Primers used are described in Table S4. The remaining *pGL4MT2* construct was digested by *Dpn I*. The 5'-prime of MRE-deletion fragments was phosphorylated by T4 polynucleotide kinase. These fragments were self-ligated by Ligation Convenience kit and transformed to DH5 α . The cloned MRE-deletion constructs were purified by QIAprep Spin Miniprep kit.

2.14. Transfection and luciferase reporter assay

Hepa1c17 cells purchased from American Type Culture Collection were maintained in DMEM, supplemented with 10% FBS, 100 U/ml penicillin, 0.01% streptomycin, 0.01% sodium pyruvate, 0.03% L-glutamine, and 55 μ M 2-mercaptoethanol at 37°C under 5.0% CO₂ condition. In the first experiment, to examine induction of *MT2* mRNA by Cd exposure, cells were seeded at a density of 4.4×10^5 cells per well in a six-well multiplate. After 24 h, cells were exposed to 5.0 μ M Cd for a specified time and harvested for qPCR analysis. In the second experiment, to study transcription activity of *MT2*, cells were seeded and incubated at a density of 4.4×10^5 cells per well in a 48-well multiplate for 24 h, followed by co-transfection with pRL-TK Vector and each *MT2* reporter construct using Lipofetamine2000 for another 24 h. Then, the cells were exposed to 5.0 or 10.0 μ M Cd for 24 h, and reporter assays were conducted using the Dual-Luciferase Reporter Assay System, following the manufacturer's instructions.

2.15. Statistical analysis

All results are expressed as mean \pm standard errors. Statistical analysis was performed using IBM SPSS Statistics ver. 19.0 (IBM). A two-way analysis of variance (ANOVA), followed by Bonferroni's post hoc test was performed to compare means of mRNA expression, histone modification, and protein expression among IU-LZ and IU-CZ or AD-LZ and AD-CZ groups of 5-week-old mice as well as reporter gene assay data. Student's *t* test was used for other analyses to compare between IU-LZ and IU-CZ groups or AD-LZ and AD-CZ groups. A *P*-value of less than .05 was considered to be statistically significant.

3. Results

3.1. Zn and Cd concentrations in liver

Pregnant mice fed the low-Zn diet had a significantly lower blood Zn concentration than those fed the control diet (3.98 ± 0.04 μ g/g, *n*=3 vs. 4.92 ± 0.10 μ g/g, *n*=6). As for the mouse progeny, no significant difference in body weight was observed between IU-LZ and IU-CZ mice on postnatal days 1, 27, and 35 (data not shown). The hepatic Zn concentration was significantly lower in 1-day-old IU-LZ mice than in IU-CZ mice (20.4 ± 1.8 μ g/g tissue, *n*=13 vs. 37.3 ± 2.9 μ g/g tissue, *n*=18), but they became similar by postnatal week 5 (Table 1). No significant changes in hepatic Zn and Cd concentrations were observed between IU-LZ and IU-CZ mice 6 h after Cd administration (Table 1).

3.2. Induction of *MT1* and *MT2* mRNAs upon Cd exposure in the liver of mice fed a Zn deficient-diet

The abundances of *MT1* and *MT2* mRNAs in the liver were examined in 5-week-old mice with and without Cd exposure. The abundances of *MT1* mRNAs in IU-LZ and IU-CZ mice at 6 h after Cd administration were significantly higher than those in the corresponding groups of mice at 0 h (Fig. 2A). Similar results to *MT1* mRNA

were observed for *MT2* mRNA although no statistically significant observations were obtained for the abundance of *MT2* mRNA in IU-CZ before and after Cd administration (Fig. 2B). Without Cd exposure, the abundances of *MT1* and *MT2* mRNAs of IU-LZ mice and those of IU-CZ mice were not different from each other (Fig. 2A, B). Six hours after Cd administration, the abundances of *MT1* mRNA was similar between IU-LZ and IU-CZ mice (Fig. 2A), whereas the abundances of *MT2* mRNA was higher in IU-LZ mice than in IU-CZ mice (Fig. 2B). Although the elevated expression of *MT* genes has been shown to be mediated by MTF1 upon Zn administration [30], no significant alterations in *MTF1* mRNA abundance were found between IU-LZ and IU-CZ mice after Cd administration (Fig. 2C).

3.3. Methyl-CpG status of *MT2* gene altered by prenatal Zn deficiency

We hypothesized that the *MT2* mRNA abundance in IU-LZ mice is enhanced by epigenetic alterations. Then, we analyzed the DNA methylation frequency by bisulfite sequencing with a special reference to the methyl-CpG status in the *MT2* promoter region and

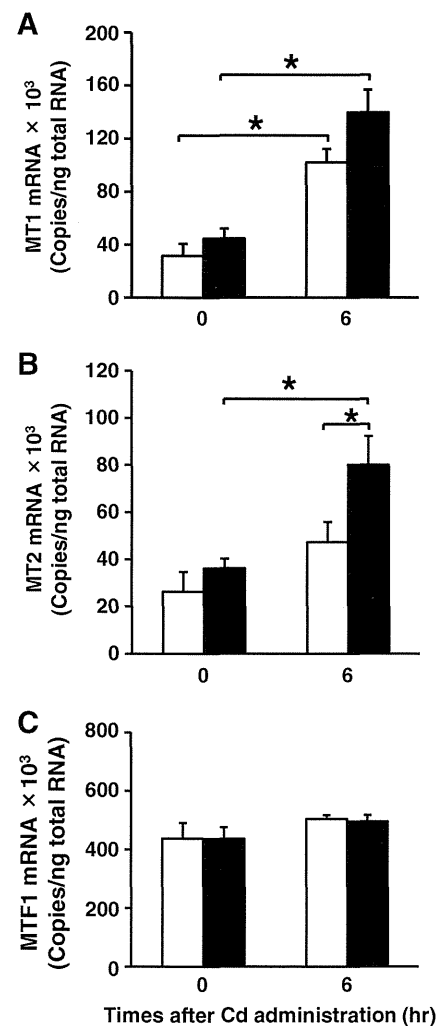


Fig. 2. Abundances of *MT1*, *MT2* and *MTF1* mRNA upon Cd exposure in liver of 5-week-old pups fed a low-Zn diet: (A) *MT1* mRNA, (B) *MT2* mRNA and (C) *MTF1* mRNA. IU-CZ (open) and IU-LZ (closed) groups. Data are expressed as mean \pm SEM (IU-CZ 0 h, *n*=5; IU-LZ 0 h, *n*=9; IU-CZ 6 h, *n*=6; IU-LZ 6 h, *n*=11). Statistically significant difference was determined by two-way ANOVA, followed by *post hoc* Bonferroni's test (**P*<.05).

Table 1

Zn and Cd concentrations in the liver of 5-week-old mice born to dams given a low-Zn diet or a control diet and those before or after Cd administration

Experimental group	Zn (μ g/g tissue)		Cd (μ g/g tissue)	
	Unexposed	Cd-exposed	Unexposed	Cd-exposed
IU-CZ	32.2 ± 0.5 (5)	42.8 ± 1.2 (6)	n. d. (5)	0.71 ± 0.13 (6)
IU-LZ	32.6 ± 0.5 (9)	42.1 ± 0.8 (11)	n. d. (9)	0.89 ± 0.11 (11)

Data are expressed as mean \pm S.E.M. with a number of animals in parentheses. n.d., not detectable.

compared the DNA methylation frequency between IU-CZ and IU-LZ mice in 5-week-old mice. The locations of the transcription start site, MREs, TATA box, and target regions amplified by primer sets are shown in Fig. 3A. The CpG islands, from the -480 to $+140$ bp region (BS-R4 and BS-R5) of the *MT2* gene, which include MREs, were not methylated in IU-CZ and IU-LZ mice. Although the vast majority of CpG

sites in the promoter region showed absolutely no methylation in either animal groups, the -834 and -820 bp CpG sites in IU-LZ mice were more frequently methylated than those in IU-CZ mice. Since the -820 bp CpG site (Fig. 3B; arrow) has the CCGC sequence that can be recognized by the methyl-sensitive restriction enzyme *Aci* I, methylation frequency analysis using *Aci* I was performed at the -820 CpG

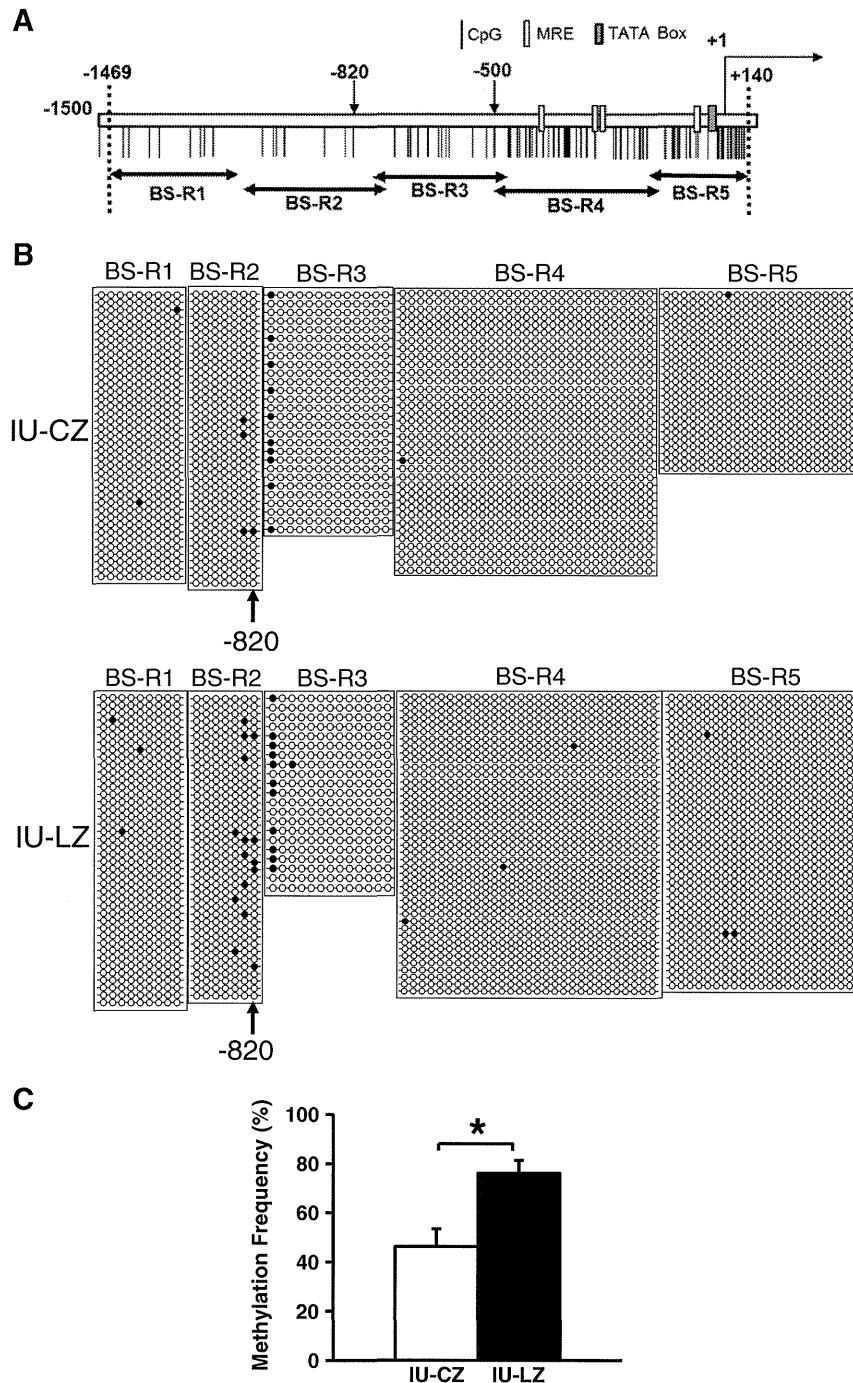


Fig. 3. Comparison of DNA methylation status and frequency of 5'-flanking region of *MT2* gene in livers of 5-week-old mice grown under perinatal Zn deficiency. (A) Target regions of *MT2* gene analyzed by bisulfite genomic sequencing. The locations of transcription start site, MREs and TATA box are shown in a previous study [50]. (B) DNA methylation status and frequency of 5'-flanking region of *MT2* of the control (IU-CZ: opened) and Zn deficiency (IU-LZ: closed) mice; CpG dinucleotides are represented by circles (●, methylated cytosine; ○, unmethylated cytosine). (C) Methylation frequency of -820 bp CpG determined by quantitative PCR with methylation-sensitive restriction enzyme. Open (IU-CZ mice) and closed (IU-LZ mice) columns are presented. Data are expressed as mean \pm S.E.M. (IU-CZ, $n=5$; IU-LZ, $n=9$). Statistically significant difference was determined by Student's *t* test ($*P<.05$).

site in the IU-CZ ($n=6$) and IU-LZ ($n=9$) mouse samples. A significant increase in DNA methylation frequency was observed at the -820 CpG site in IU-LZ mouse samples, suggesting the association of prenatal Zn deficiency with a high methylation status (Fig. 3C), which is consistent with the result of bisulfite sequencing (Fig. 3B).

3.4. *MT2* promoter analysis

No data on *MT2* promoter functional analysis in various animal species is available. Thus, using an *MT2* gene-promoter-driven luciferase reporter gene assay, we confirmed that *MT2* mRNA abundances were significantly induced in Hepa1c1c7 cells as early as 3 h after Cd addition to the medium (Fig. 4A). For deletion analysis, we made six deletion constructs from an original construct connected with a 2,166 bp flanking region to the pGL4 vector (*pGL4MT2-2166*), on the basis of the strategy that the possible functionalities of the four MREs can be evaluated (Fig. 4B). Hepa1c1c7 cells that were transfected with either of the *pGL4MT2-2166*, *pGL4MT2-397*, *pGL4MT2-307* or *pGL4MT2-287* construct were found to have significantly elevated transcription activity upon exposure to 5.0 or 10.0 μM Cd (Fig. 4B). However, almost no additional induction above a constitutive level was observed by Cd treatment in the following three transfected cell lines: cells transfected with *pGL4MT2 Δ -397-37* construct from which all four MRE motifs were deleted, those transfected with *pGL4MT2-65* having an MRE motif and those transfected with *pGL4MT2-37* having no MRE motif (Fig. 4B). Collectively, only one MRE located between a -287 to -65 bp

region are suggested to play a crucial role in the induction of *MT2* mRNA by Cd in these cells.

3.5. Histone modifications of *MT2* gene altered by prenatal Zn deficiency

We applied the ChIP assay to the four target regions (Ch-R1, Ch-R2, Ch-R3 and Ch-R4) of the *MT2* promoter regions, in 5-week-old mice, which contain MREs or -820 CpG, to examine whether histone modifications are altered by the Zn status in the prenatal period (Fig. 5A). We found that the basal amounts of AcH3 at Ch-R1 and Ch-R3, AcH4 at Ch-R1 and Ch-R2 and AcH3K14 at Ch-R3 in IU-LZ mice are significantly higher than those in IU-CZ mice (Fig. 5B, C and E). In Cd-exposed mice, histone modification levels in IU-LZ mice in comparison with those in IU-CZ mice were significantly increased: AcH3 (Fig. 5B) and AcH4 (Fig. 5C) levels in Ch-R2, Ch-R3, and Ch-R4; AcH3K9 (Fig. 5D) levels at Ch-R2 and Ch-R3; AcH3K14 levels in Ch-R1, Ch-R2, Ch-R3 and Ch-R4 (Fig. 5E); and H3K4me3 levels at Ch-R3 (Fig. 5F).

In IU-LZ mice, Cd administration significantly increased the AcH3K14 levels at Ch-R1 and Ch-R2 (Fig. 5E) and H3K4me3 levels at Ch-R3 (Fig. 5F), whereas it significantly decreased the AcH3 (Fig. 5B) and AcH4 (Fig. 5C) levels at Ch-R1. It is not known why Cd exposure reduced histone acetylation in the Ch-R1 region. However, this region is not considered to be responsible for transcription. Next, to determine whether these histone modifications occurred in the newborn livers, we analyzed *MT2* promoter regions in the liver from the 1-day-old pups born to dams given a Zn deficient diet during gestation. The abundances of *MT1*, *MT2* and *MTF1* mRNAs in IU-LZ

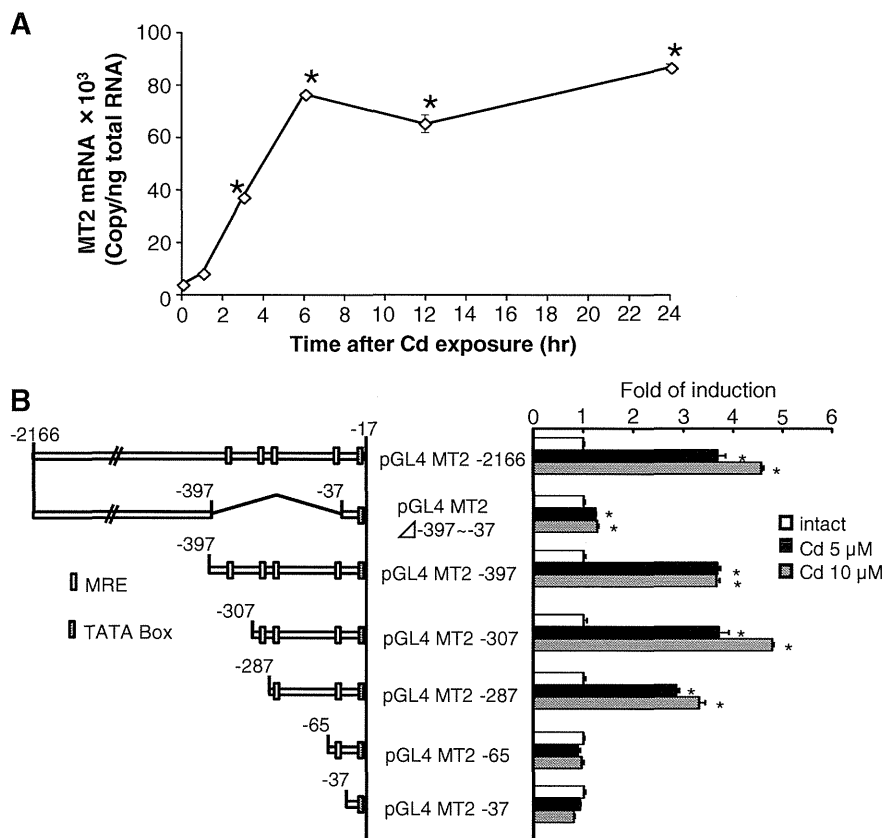


Fig. 4. *MT2* promoter analysis using reporter gene assay. (A) Abundance of *MT2* mRNA in Hepa1c1c7 cells at 0, 3, 6, 12 and 24 h after 5.0 μM Cd treatment. Data are expressed as mean \pm S.E.M. ($n=3$ per group). Statistically significant difference was determined by one-way ANOVA, followed by post hoc Bonferroni's test ($*P<.05$ vs. 0 h). (B) Structure of *MT2* MRE-deletion constructs (left). Reporter gene activity in Hepa1c1c7 cells transfected with *MT2* MRE-deletion constructs at 24 h after 5.0 and 10.0 μM Cd treatment (right). Data are expressed as mean \pm S.E.M. ($n=3$ per group). Statistically significant difference was determined by one-way ANOVA, followed by post hoc Bonferroni's test at each construct ($*P<.05$ vs. intact).

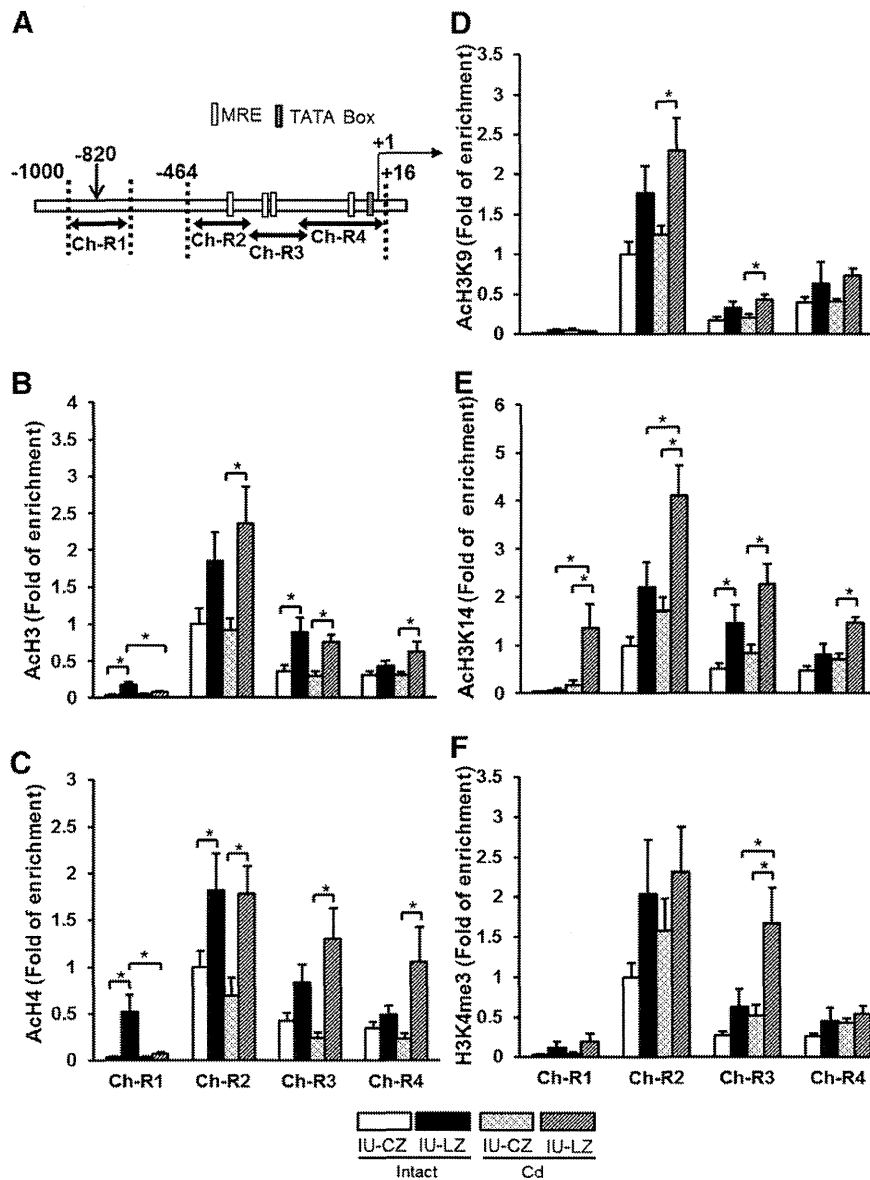


Fig. 5. Changes in histone modification levels in *MT2* promoter regions in 5-week-old mice grown under prenatal Zn deficiency. The livers were collected before and 6 h after Cd administration. (A) Target regions of *MT2* promoter for ChIP assay and localizations of transcription start site, MREs and TATA box are shown in a previous study [50]. Changes in levels of (B) acetylated histone H3, (C) acetylated histone H4, (D) acetylated histone H3 lysine 9, (E) acetylated histone H3 lysine 14, and (F) tri-methylated histone H3 lysine 4. Open (IU-CZ intact mice), closed (IU-LZ intact mice), dotted (IU-CZ Cd-exposed mice), and diagonal (IU-LZ Cd-exposed mice) columns are presented. Data are expressed as mean \pm S.E.M. ($n=8$ per group). Statistically significant difference was determined by two-way ANOVA, followed by post hoc Bonferroni's test at each region ($*P<0.05$).

mice was not altered in comparison with those in IU-CZ mice (Fig. 6A). The AcH3 levels at Ch-R2 and Ch-R3 were significantly higher in IU-LZ mice than in IU-CZ mice (Fig. 6B). The AcH4 levels at Ch-R2 in IU-LZ mice tended to increase in comparison with those in IU-CZ mice (Fig. 6C). These results suggest that the histone acetylation level was already initiated to increase during the perinatal stage by the Zn deficiency *in utero*.

3.6. Zn deficiency *in utero* prolonged MTF1 binding to the *MT2* promoter region upon Cd administration

Since the epigenetic alterations as shown in the previous section suggested the loosening of the chromatin structure in the *MT2* promoter region, we investigated whether Cd exposure *in vivo* affects

the status of MTF1 binding to a particular region (Ch-R1, Ch-R2, Ch-R3, and Ch-R4) in the *MT2* promoter by the ChIP assay (Table 2). The amounts of MTF1 bound to Ch-R2, Ch-R3 and Ch-R4 were greater at 1 h than those at 0 and 6 h after Cd administration in all the animals (Table 2). The amount of MTF1 bound to Ch-R1, which does not have an MRE motif, was not detected at these time points (data not shown).

The amounts of MTF1 bound to Ch-R3 and Ch-R4, but not Ch-R2 were observed to be significantly higher in IU-LZ mice than in IU-CZ mice 6 h after Cd administration, whereas no difference in the amounts of MTF1 bound to these regions was found between the IU-CZ and IU-LZ mice 1 h after Cd administration, which suggests the prolongation of MTF1 binding to the MRE motif (Table 2). The amounts of MTF1 protein in both nucleus and cytosol were unchanged between the IU-LZ and IU-CZ mice and between before

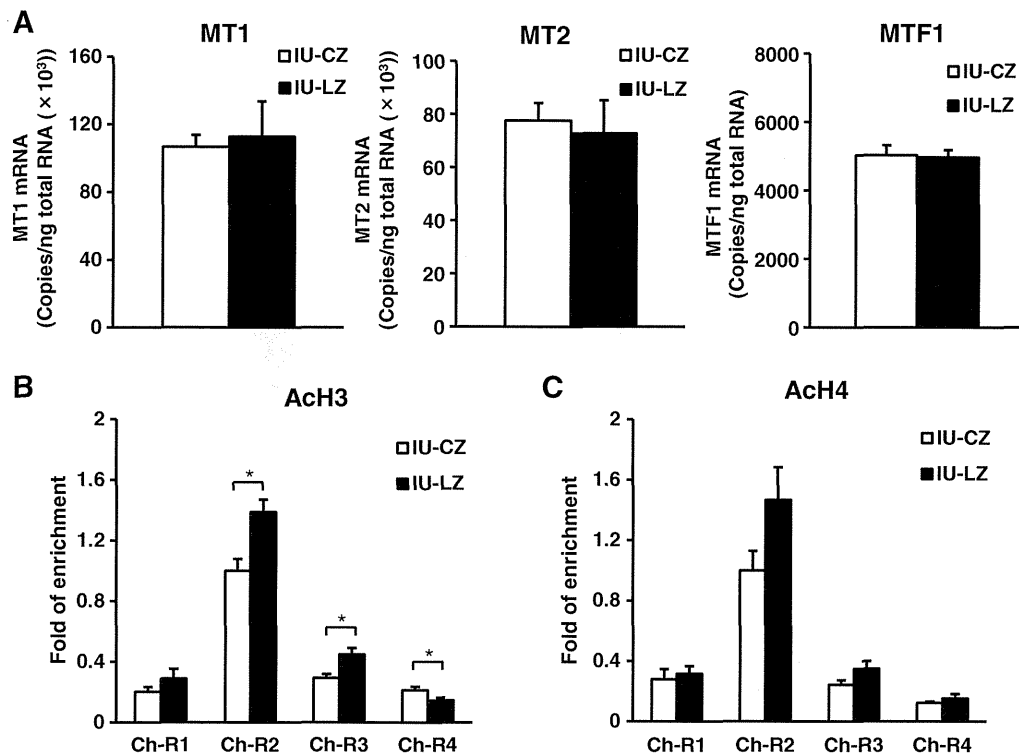


Fig. 6. (A) Abundances of *MT1*, *MT2* and *MTF1* mRNAs and (B) levels of acetylated histone H3 and (C) histone H4 in the *MT2* gene in the liver in 1-day-old male pups grown under Zn deficiency condition. The target regions for histone modifications analysis are shown in Fig. 5A. Data are expressed as mean \pm S.E.M. ($n=6$ per group). Statistically significant difference was determined by Student's *t* test at each region (* $P<.05$).

and 6 h after Cd administration (Fig. 7), suggesting that the total amounts of MTF1 protein in the liver were not altered by prenatal Zn deficiency or Cd administration.

3.7. Epigenetic alterations induced by Zn-deficiency in adulthood

To determine whether the epigenetic alterations induced by Zn deficiency are a temporally specific event, adult mice were fed a low-Zn diet or a control diet for 12 days, and the liver was collected just after the end of this period and subjected to the epigenetic analyses. In the AD-CZ and AD-LZ mice, no significant differences in the mRNA abundances of *MT1*, *MT2* and *MTF1* were found (Fig. 8A). Although the levels of ACh3 (Fig. 8B) and ACh3K14 (Fig. 8E) at Ch-R1 in the *MT2* promoter of AD-LZ mice were significantly higher than those of AD-CZ mice, the differences were not conspicuous. No significant differences in the amounts of other histone modifications in ACh4 (Fig. 8C), ACh3K9 (Fig. 8D) and H3K4me3 (Fig. 8F) were found between AD-LZ and AD-CZ mice. In addition, the DNA methylation frequency at a -820 bp CpG site in the *MT2* promoter of AD-LZ mice was not different from that of the AD-CZ mice (Fig. 8G).

Next, to study the possible involvement of Zn deficiency in the inducibilities of *MT1/2* mRNAs, the Zn-deficient diet was replaced with a regular diet, and the inducibilities of *MT1* and *MT2* mRNAs by Cd administration were examined one month later. Under this condition, no difference in *MT1* and *MT2* mRNA abundances was observed between the AD-LZ and AD-CZ mice 6 h after Cd administration (Fig. 8H). The *MTF1* mRNA abundance was significantly lower in AD-LZ mice than in the AD-CZ mice (Fig. 8I).

Collectively, epigenetic alterations of the *MT2* gene were found to be caused by Zn deficiency during the prenatal period, but not in adulthood.

4. Discussion

A remarkable finding of this study is that epigenetic alterations of the promoter of the *MT2* gene under prenatal Zn deficiency condition are associated with a significant enhancement of Cd-dependent induction of *MT2* mRNA in the liver of mouse progeny later in adulthood. The first question that was addressed is when such epigenetic alterations occur and how long they last. In the 5-week-old

Table 2
Amounts of MTF1 bound to *MT2* promoter post Cd administration in the liver of 5-week-old mice born to dams fed a low-Zn diet or a control diet

Target region	Ch-R2			Ch-R3			Ch-R4		
	0	1	6	0	1	6	0	1	6
	Fold of enrichment								
IU-CZ	1.00 \pm 0.29	9.13 \pm 3.44	0.74 \pm 0.23	1.00 \pm 0.45	6.21 \pm 1.60	0.65 \pm 0.18	1.00 \pm 0.31	3.24 \pm 1.08	0.32 \pm 0.06
IU-LZ	0.69 \pm 0.25	9.17 \pm 2.76	0.45 \pm 0.10	0.54 \pm 0.20	8.00 \pm 3.69	1.54 \pm 0.25*	0.78 \pm 0.19	3.30 \pm 1.25	1.16 \pm 0.30*

Each target regions are the ones shown in Fig. 5A. Data are expressed as mean \pm S.E.M. ($n=6$ per group). Statistically significant difference between IU-CZ and IU-LZ mice by Student's *t*-test (* $P<.05$).

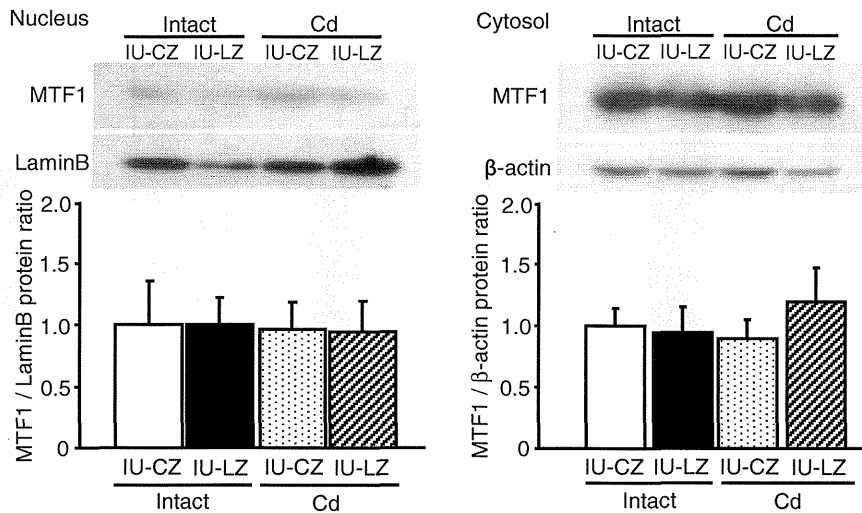


Fig. 7. Amounts of hepatic MTF1 protein in 5-week-old pups grown under Zn deficiency condition. The livers were collected before and 6 h after Cd administration. Scanning densitometry was used for semi quantitative analysis. Data are expressed as mean \pm S.E.M. ($n=5$ per group).

IU-LZ mice, significant increases in DNA methylation frequency at the -820 CpG site and histone modifications were demonstrated in comparison with those in IU-CZ mouse progeny. However, this region is not considered to be responsible for transcription. To examine when these histone modifications were caused by Zn deficiency, we analyzed the *MT2* promoter region in the liver from the 1-day-old pups born to dams given a Zn-deficient diet during gestation. Collectively, the IU-LZ mice had significantly elevated Ach3 levels at Ch-R2 and Ch-R3 and showed a tendency of Ach4 levels to increase at Ch-R2 in comparison with IU-CZ mice, suggesting that histone acetylation levels were increased during the prenatal stage. Taken together, zinc deficiency *in utero* alters fetal histone modifications, and these changes are being stored as an epigenetic memory until adulthood (Supplemental Fig. 1). In this study, we could not provide direct evidence on molecular mechanisms by which histone modification enhance Cd-induced *MT2* mRNA expression in IU-LZ mice. However, the elevation in histone acetylation observed in the IU-LZ mice is considered to keep the nucleosome in an “open chromatin” state [38]. Therefore, it is likely that p300 and Sp1 that are known to be recruited by MTF1 [30] will easily make an access to the *MT2* promoter region under the open chromatin condition and that Cd-induced *MT2* mRNA abundance is enhanced in IU-LZ mice. Further studies will be required to reveal the molecular mechanisms how prenatal Zn deficiency regulates not only gene expression via histone modifications, but also maintain histone modifications.

The next question was whether the epigenetic alterations are more specifically induced by Zn deficiency *in utero* rather than in adulthood. When adult mice fed a low-Zn diet (AD-LZ) or those fed a control diet (AD-CZ) were compared, the levels of Ach3/Ach3K14 of the *MT2* gene at Ch-R1 in AD-LZ mice were significantly different from those in AD-CZ mice. However, these changes did not seem to contribute to the alteration of the induction of *MT2* transcription following Cd exposure, because the Ch-R1 region is considered to be irrelevant to transcription (Fig. 4). In addition, the induction of *MT2* mRNA by Cd exposure in AD-LZ mice was not different from that in AD-CZ mice (Fig. 8H). Therefore, it is not likely that the alteration of histone modifications induced by Zn deficiency played a significant role to induce *MT2* mRNA upon Cd exposure in AD-LZ mice. Our results clearly show that mouse fetuses are more responsive to Zn deficiency resulting in epigenetic alterations than adult mice. On the other hand, epigenetic alterations are known to be caused by environmental factors in adulthood as well. Examples of this are an

increase in DNA methylation levels of tumor-suppressor genes, such as p16, in the stomach following infection by *Helicobacter pylori* in humans [39,40], DNA hypomethylation of *Ppary* in mice fed a high-fat diet [41] and DNA hypermethylation of *PPlc* and DNA hypomethylation of *fosB* in nucleus accumbens in cocaine-administered mice [42]. In the case of the nutritional status of Zn, significant epigenetic alterations might occur when adult animals are exposed to extremely low Zn levels for a longer time than under the present experimental conditions.

The other question is how Cd administration enhanced the *MT2* induction in IU-LZ mice compared with IU-CZ mice later in life. A plausible explanation is that the prenatal Zn deficiency induced enhanced histone modifications in the *MT2* promoter region that includes MREs, and that MTF1 or yet-undefined transcription factors may have easy access to the MRE motif to activate the *MT2* gene expression upon Cd or Zn exposure. This conjecture was supported by the elevated levels of acetylated histones and methylated H3K4 in the *MT2*-400 bp 5' flanking region in the IU-LZ mice compared with those in the IU-CZ mice (Fig. 5). It is reasonable to think that such an open-chromatin structure persists into adulthood and allows transcription to be activated, as has been reported for other genes such as *Hoxa10* or *Gfap* [43,44]. On the other hand, because of the lack of MRE motifs, it is less likely that the change in DNA methylation frequency at -820 bp CpG in the *MT2* promoter region in the IU-LZ mice is associated with the enhanced *MT2* gene expression later in life (Fig. 3).

MTF1 binding to the MRE motif in the *MT1* gene has been proposed to play an important role in the induction of this gene [30]. Although no data are available on the interaction of MTF1 with the *MT2* gene, our reporter gene assay (Fig. 4) and ChIP assay (Table 2) results suggested that MTF1 can bind to the MRE motif in the *MT2* gene. The significantly prolonged MTF1 binding 6 h after Cd administration in the IU-LZ mice (Table 2) may explain the enhanced *MT2* mRNA induction: That is, it is conceivable that the highly acetylated state of histones bound to the DNA fragment adjacent to MREs (Fig. 5) affects the three-dimensional interaction between the MTF1 protein and DNA, and that the net dissociation of MRE with MTF1 may be reduced owing to structural changes in the nucleosome. As described above, the possible removal or slide of histone H3 in *MT1* promoter by Zn treatment may have an interaction with MTF1, and the binding of MTF1 to the promoter is required to initiate the exclusion of histone [45]. Thus, it can be speculated that the

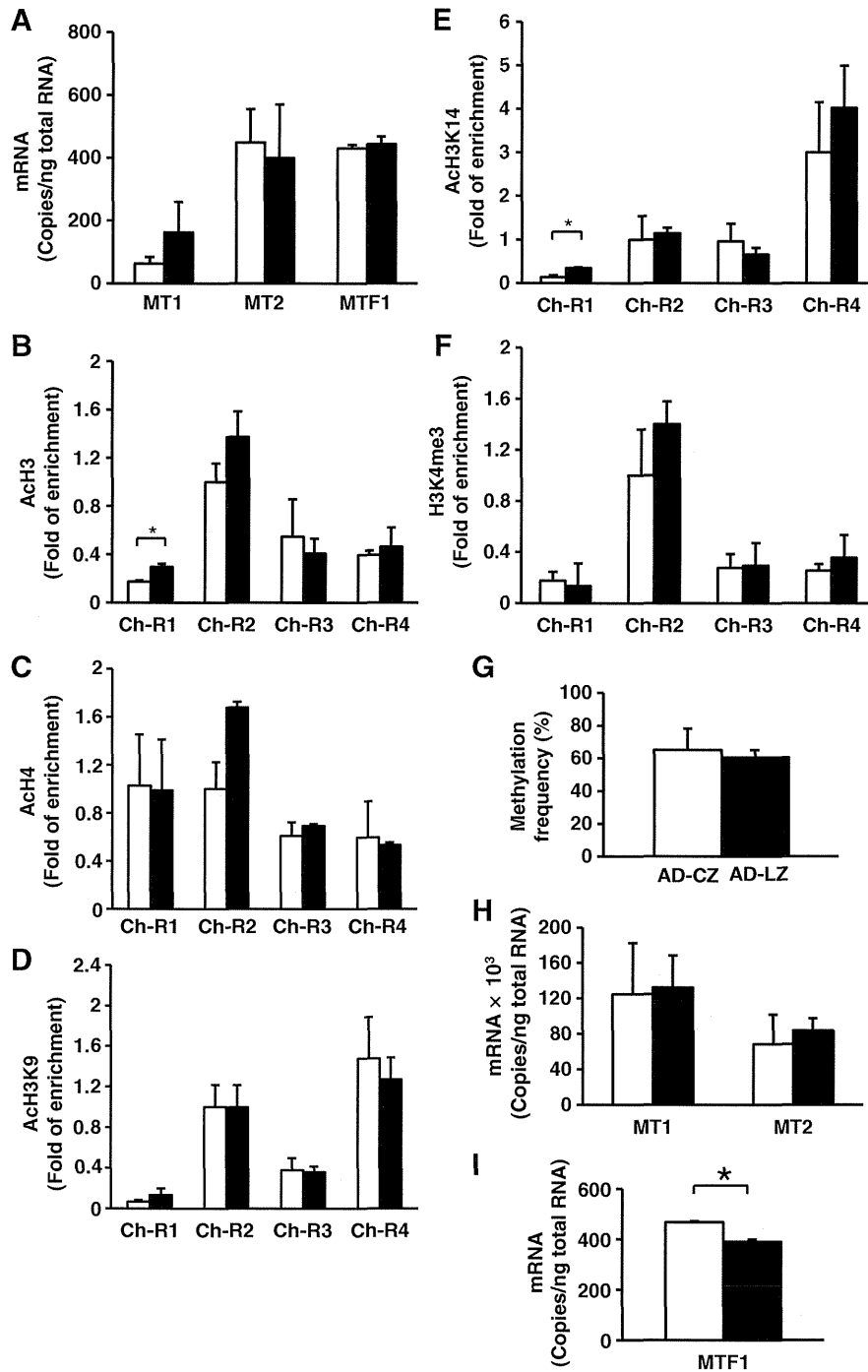


Fig. 8. Abundances of *MT1*, *MT2* and *MTF1* mRNAs, and histone modification in the *MT2* promoter of liver from mice fed a low-Zn diet for 12 days in adulthood (A–G), or those fed with a low-Zn diet followed by a regular diet for a month in adulthood (H–I). (A) *MT1*, *MT2* and *MTF1* mRNAs. (B) Acetylated histone H3. (C) Acetylated histone H4. (D) Acetylated histone H3 lysine 9. (E) Acetylated histone H3 lysine 14. (F) Tri-methylated histone H3 lysine 4. (G) Methylation frequency of –820 bp CpG included in *Aci* I site. See legend to Fig. 5A for target regions of histone modifications. Data on hepatic *MT1* and *MT2* (H) and *MTF1* mRNA (I) were obtained 6 h after oral administration of Cd at 5.0 mg kg⁻¹ b.w. Open (AD-CZ mice) and closed (AD-LZ mice) columns are presented. Data are expressed as mean ± S.E.M. ($n=3$ per group). Statistically significant difference was determined by Student's *t* test (* $P<.05$).

prolonged binding of *MTF1* to *MT2* promoter in IU-LZ mice may be involved in the maintenance of the opened chromatin structure.

Another question to be addressed is what the enhanced *MT2* mRNA induction in adulthood caused by *in utero* Zn deficiency indicates. It has been reported that abnormal morphogenesis occurred in the *MT1/2*-null fetus grown under Zn deficiency *in utero* [46]. On the contrary, this effect was prevented in the transgenic mice

over expressing the *MT1* protein [47]. *MT1/2* null mice fed a low-Zn diet for 3 weeks from birth developed swollen Bowman's space in the kidney in comparison with wild-type mice [48]. These studies suggest that *MT1/2* proteins protect against Zn deficiency. It can be speculated from our study that mice grown under prenatal Zn deficiency maintain the inducibility of *MT2* mRNA as an epigenetic memory in the genome. In this case, it is thought that mice can be prepared for Zn

deficiency that they may encounter in the future, and that they will be able to efficiently respond to the low-Zn condition. This idea could be supported by an analogy to the thrifty phenotype hypothesis in that neonates who experienced poor nutrition *in utero* have metabolic adaptations that emerge in anticipation of a low-quality adult breeding environment [49].

In conclusion, the present study demonstrates for the first time that prenatal Zn deficiency causes epigenetic alterations in the liver of offspring. The enhanced *MT2* gene induction by metal exposure after birth is considered to be due to epigenetic alterations, such as enhanced acetylation levels of histones bound to approximately –400 bp of the *MT2*-5′ flanking region. Histone modifications caused by Zn deficiency during the early-developmental period may persist into adulthood as an epigenetic memory. The results of the present study results could also support the DOHaD hypothesis from the perspective that a particular nutrition factor such as an essential trace element during prenatal period can affect epigenome of children.

Acknowledgments

We thank Dr. Chiho Watanabe (Department of Human Ecology, Graduate School of Medicine, The University of Tokyo) for useful suggestions on the result of our experiments, and colleagues in our laboratory for constructive comments.

Appendix A. Supplementary data

Supplementary data to this article can be found online at <http://dx.doi.org/10.1016/j.jnutbio.2012.05.013>.

References

- Painter RC, Roseboom TJ, Bleker OP. Prenatal exposure to the Dutch famine and disease in later life: an overview. *Reprod Toxicol* 2005;20:345–52.
- Barker DJ, Winter PD, Osmond C, Margetts B, Simmonds SJ. Weight in infancy and death from ischaemic heart disease. *Lancet* 1989;2:577–80.
- Barker DJ, Osmond C, Golding J, Kuh D, Wadsworth ME. Growth in utero, blood pressure in childhood and adult life, and mortality from cardiovascular disease. *BMJ* 1989;298:564–7.
- Forsen T, Eriksson JG, Tuomilehto J, Osmond C, Barker DJ. Growth in utero and during childhood among women who develop coronary heart disease: longitudinal study. *BMJ* 1999;319:1403–7.
- Gillman MW, Barker D, Bier D, Gagampang F, Challis J, Fall C, et al. Meeting report on the 3rd International Congress on Developmental Origins of Health and Disease (DOHaD). *Pediatr Res* 2007;61:625–9.
- Torrens C, Poston L, Hanson MA. Transmission of raised blood pressure and endothelial dysfunction to the F2 generation induced by maternal protein restriction in the F0, in the absence of dietary challenge in the F1 generation. *Br J Nutr* 2008;100:760–6.
- Burdge GC, Slater-Jefferies J, Torrens C, Phillips ES, Hanson MA, Lillycrop KA. Dietary protein restriction of pregnant rats in the F0 generation induces altered methylation of hepatic gene promoters in the adult male offspring in the F1 and F2 generations. *Br J Nutr* 2007;97:435–9.
- Simmons RA, Templeton LJ, Gertz SJ. Intrauterine growth retardation leads to the development of type 2 diabetes in the rat. *Diabetes* 2001;50:2279–86.
- Park JH, Stoffers DA, Nicholls RD, Simmons RA. Development of type 2 diabetes following intrauterine growth retardation in rats is associated with progressive epigenetic silencing of *Pdx1*. *J Clin Invest* 2008;118:2316–24.
- Bernal AJ, Jirtle RL. Epigenomic disruption: the effects of early developmental exposures. *Birth Defects Res A Clin Mol Teratol* 2010;88:938–44.
- Newbold RR, Padilla-Banks E, Jefferson WN, Heindel JJ. Effects of endocrine disruptors on obesity. *Int J Androl* 2008;31:201–8.
- Waterland RA, Travasano M, Tahiliani KG. Diet-induced hypermethylation at agouti viable yellow is not inherited transgenerationally through the female. *FASEB J* 2007;21:3380–5.
- Jones PA, Bayliss SB. The fundamental role of epigenetic events in cancer. *Nat Rev Genet* 2002;3:415–28.
- Jenuwein T, Allis CD. Translating the histone code. *Science* 2001;293:1074–80.
- Anway MD, Cupp AS, Uzumcu M, Skinner MK. Epigenetic transgenerational actions of endocrine disruptors and male fertility. *Science* 2005;308:1466–9.
- Tomat AL, Insera F, Veiras L, Vallone MC, Balaszczuk AM, Costa MA, et al. Moderate zinc restriction during fetal and postnatal growth of rats: effects on adult arterial blood pressure and kidney. *Am J Physiol Regul Integr Comp Physiol* 2008;295:R543–9.
- Halas ES, Eberhardt MJ, Diers MA, Sandstead HH. Learning and memory impairment in adult rats due to severe zinc deficiency during lactation. *Physiol Behav* 1983;30:371–81.
- Halas ES, Hunt CD, Eberhardt MJ. Learning and memory disabilities in young adult rats from mildly zinc deficient dams. *Physiol Behav* 1986;37:451–8.
- Beach RS, Gershwin ME, Hurley LS. Gestational zinc deprivation in mice: persistence of immunodeficiency for three generations. *Science* 1982;218:469–71.
- Tuerk MJ, Fazel N. Zinc deficiency. *Curr Opin Gastroenterol* 2009;25:136–43.
- Vallée BL, Falchuk KH. The biochemical basis of zinc physiology. *Physiol Rev* 1993;73:79–118.
- Hunt JR. Bioavailability of iron, zinc, and other trace minerals from vegetarian diets. *Am J Clin Nutr* 2003;78:633S–9S.
- Wastney ME, Ahmed S, Henkin RI. Changes in regulation of human zinc metabolism with age. *Am J Physiol* 1992;263:R1162–8.
- Menzano E, Carlen PL. Zinc deficiency and corticosteroids in the pathogenesis of alcoholic brain dysfunction – a review. *Alcohol Clin Exp Res* 1994;18:895–901.
- Jeejeebhoy K. Zinc: an essential trace element for parenteral nutrition. *Gastroenterology* 2009;137:57–12.
- Fischer Walker CL, Ezzati M, Black RE. Global and regional child mortality and burden of disease attributable to zinc deficiency. *Eur J Clin Nutr* 2009;63:591–7.
- Coyle P, Philcox JC, Carey LC, Rofe AM. Metallothionein: the multipurpose protein. *Cell Mol Life Sci* 2002;59:627–47.
- Nies DH. Microbial heavy-metal resistance. *Appl Microbiol Biotechnol* 1999;51:730–50.
- Solis WA, Childs NL, Weedon MN, He L, Nebert DW, Dalton TP. Retrovirally expressed metal response element-binding transcription factor-1 normalizes metallothionein-1 gene expression and protects cells against zinc, but not cadmium, toxicity. *Toxicol Appl Pharmacol* 2002;178:93–101.
- Li Y, Kimura T, Huyck RW, Laity JH, Andrews GK. Zinc-induced formation of a coactivator complex containing the zinc-sensing transcription factor MTF-1, p300/CBP, and Sp1. *Mol Cell Biol* 2008;28:4275–84.
- Vruwink KG, Hurley LS, Gershwin ME, Keen CL. Gestational zinc deficiency amplifies the regulation of metallothionein induction in adult mice. *Proc Soc Exp Biol Med* 1988;188:30–4.
- Tomat AL, Insera F, Veiras L, Vallone MC, Balaszczuk AM, Costa MA, et al. Moderate zinc restriction during fetal and postnatal growth of rats: effects on adult arterial blood pressure and kidney. *Am J Physiol Regul Integr Comp Physiol* 2008;295:R543–9.
- Wang FD, Bian W, Kong LW, Zhao FJ, Guo JS, Jing NH. Maternal zinc deficiency impairs brain nestin expression in prenatal and postnatal mice. *Cell Res* 2001;11:135–41.
- Oteiza PI, Hurley LS, Lonnerdal B, Keen CL. Marginal zinc deficiency affects maternal brain microtubule assembly in rats. *J Nutr* 1988;118:735–8.
- Shiizaki K, Ohsako S, Koyama T, Nagata R, Yonemoto J, Tohyama C. Lack of CYP1A1 expression is involved in unresponsiveness of the human hepatoma cell line SK-HEP-1 to dioxin. *Toxicol Lett* 2005;160:22–33.
- Clark SJ, Harrison J, Paul CL, Frommer M. High sensitivity mapping of methylated cytosines. *Nucleic Acids Res* 1994;22:2990–7.
- Lee TI, Johnstone SE, Young RA. Chromatin immunoprecipitation and microarray-based analysis of protein location. *Nat Protoc* 2006;1:729–48.
- Kouzarides T. Chromatin modifications and their function. *Cell* 2007;128:693–705.
- Maekita T, Nakazawa K, Mihara M, Nakajima T, Yanaoka K, Iguchi M, et al. High levels of aberrant DNA methylation in *Helicobacter pylori*-infected gastric mucosae and its possible association with gastric cancer risk. *Clin Cancer Res* 2006;12:989–95.
- Nakajima T, Maekita T, Oda I, Gotoda T, Yamamoto S, Umemura S, et al. Higher methylation levels in gastric mucosae significantly correlate with higher risk of gastric cancers. *Cancer Epidemiol Biomarkers Prev* 2006;15:2317–21.
- Fujiki K, Kano F, Shiota K, Murata M. Expression of the peroxisome proliferator activated receptor gamma gene is repressed by DNA methylation in visceral adipose tissue of mouse models of diabetes. *BMC Biol* 2009;7:38.
- Anier K, Malinovskaja K, Aonurm-Helm A, Zharkovskiy A, Kalda A. DNA methylation regulates cocaine-induced behavioral sensitization in mice. *Neuropsychopharmacology* 2010;35:2450–61.
- Bromer JG, Zhou Y, Taylor MB, Doherty L, Taylor HS. Bisphenol-A exposure in utero leads to epigenetic alterations in the developmental programming of uterine estrogen response. *FASEB J* 2010;24:2273–80.
- Asano H, Aonuma M, Sanosaka T, Kohyama J, Namihira M, Nakashima K. Astrocyte differentiation of neural precursor cells is enhanced by retinoic acid through a change in epigenetic modification. *Stem Cells* 2009;27:2744–52.
- Okumura F, Li Y, Itoh N, Nakanishi T, Isobe M, Andrews GK, et al. The zinc-sensing transcription factor MTF-1 mediates zinc-induced epigenetic changes in chromatin of the mouse metallothionein-I promoter. *Biochim Biophys Acta* 2011;1809:56–62.
- Andrews GK, Geiser J. Expression of the mouse metallothionein-I and -II genes provides a reproductive advantage during maternal dietary zinc deficiency. *J Nutr* 1999;129:1643–8.
- Dalton T, Fu K, Palmiter RD, Andrews GK. Transgenic mice that overexpress metallothionein-I resist dietary zinc deficiency. *J Nutr* 1996;126:825–33.
- Kelly EJ, Quaipe CJ, Froelick CJ, Palmiter RD. Metallothionein I and II protect against zinc deficiency and zinc toxicity in mice. *J Nutr* 1996;126:1782–90.
- Wells JC. The thrifty phenotype hypothesis: thrifty offspring or thrifty mother? *J Theor Biol* 2003;221:143–61.
- Searle PF, Davison BL, Stuart GW, Wilkie TM, Norstedt G, Palmiter RD. Regulation, linkage, and sequence of mouse metallothionein I and II genes. *Mol Cell Biol* 1984;4:1221–30.

Prenatal Exposure to Permethrin Influences Vascular Development of Fetal Brain and Adult Behavior in Mice Offspring

Satoshi Imanishi,¹ Masahiro Okura,¹ Hiroko Zaha,¹ Toshifumi Yamamoto,²
Hiromi Akanuma,¹ Reiko Nagano,¹ Hiroaki Shiraiishi,¹ Hidekazu Fujimaki,¹ Hideko Sone¹

¹Health Risk Research Section, Center for Environmental Risk Research, National Institute for Environmental Studies 16-2, Onogawa, Tsukuba, Ibaraki 305-8506, Japan

²Laboratory of Molecular Recognition, Graduate School of Nanosciences, Yokohama City University, 22-2 Seto, Kanazawa-ku, Yokohama 236-0027, Japan

Received 14 April 2011; revised 17 June 2011; accepted 25 June 2011

ABSTRACT: Pyrethroids are one of the most widely used classes of insecticides and show neurotoxic effects that induce oxidative stress in the neonatal rat brain. However, little is still known about effects of prenatal exposure to permethrin on vascular development in fetal brain, central nervous system development, and adult offspring behaviors. In this study, the effects of prenatal exposure to permethrin on the development of cerebral arteries in fetal brains, neurotransmitter in neonatal brains, and locomotor activities in offspring mice were investigated. Permethrin (0, 2, 10, 50, and 75 mg/kg) was orally administered to pregnant females once on gestation day 10.5. The brains of permethrin-treated fetuses showed altered vascular formation involving shortened lengths of vessels, an increased number of small branches, and, in some cases, insufficient fusion of the anterior communicating arteries in the area of circle of Willis. The prenatal exposure to permethrin altered neocortical and hippocampus thickness in the mid brain and significantly increased norepinephrine and dopamine levels at postnatal day 7 mice. For spontaneous behavior, the standing ability test using a viewing jar and open-field tests showed significant decrease of the standing ability and locomotor activity in male mice at 8 or 12 weeks of age, respectively. The results suggest that prenatal exposure to permethrin may affect insufficient development of the brain through alterations of vascular development. © 2011 Wiley Periodicals, Inc. *Environ Toxicol* 28: 617–629, 2013.

Keywords: pyrethroids; cerebral arteries; fetal exposure; mice

INTRODUCTION

Permethrin, a member of the synthetic pyrethroid family, is widely used to control insect pests in agricultural, residential, and other applications as well as for avoiding malaria. Residentially, people may be exposed through pest control operations and contaminated food and water (Gorell et al., 1998). Preschool children have been found to be potentially

exposed to permethrin from several sources and through several routes in their daily environments (Tulve et al., 2006; Morgan et al., 2007; Naeher et al., 2009). Permethrin is also known as a neurotoxin (Imamura et al., 2000; Meyer et al., 2008; Shafer et al., 2008). Pyrethroids target neuronal sodium channels, increasing sodium entry into nerve cells and inducing depolarization of nerve membranes and blockage of nerve conduction at high concentrations (Narahashi, 1996). Reactive oxygen species have also been implicated in the toxicology of permethrin. In neonatal rats, behavioral changes, alterations in striatal monoamine levels, and striatal protein oxidation have been reported

Correspondence to: H. Sone; e-mail: hsone@nies.go.jp

Published online 24 August 2011 in Wiley Online Library (wileyonlinelibrary.com). DOI 10.1002/tox.20758

(Cantalamessa, 1993; Gabbianelli et al., 2002; Nasuti et al., 2003), and adult animals exposed to permethrin show abnormalities or degeneration of dopaminergic nerve pathways (Karen et al., 2001; Bloomquist et al., 2002; Gillette and Bloomquist, 2003; Jortner, 2006). Indeed, a mixture of the antioxidant vitamins C and E suppressed pyrethroid toxicity, suggesting that these antioxidants could protect the erythrocyte plasma membrane against the oxidative injury induced by pyrethroid exposure (Gabbianelli et al., 2004). Pups from mice administered permethrin before mating are inhibited in behavioral development (Farak et al., 2006), and neonatal exposure to permethrin alters levels of oxidative-damage molecular markers and dopaminergic locomotor behavior later in adults (Nasuti et al., 2008). Thus, prenatal exposure to permethrin induces neurotoxicity as it does in adults.

The neurotoxicity of permethrin and other pyrethroids has been thought to contribute to neurodegenerative diseases like Parkinson's disease and Alzheimer's disease as well as cognitive impairment (Nasuti et al., 2008), because oxidative stress is a common event of biological impairment in brain aging and neurodegenerative and vascular disease.

Vascular development is essential for a variety of physiological events, and abnormalities in vascular development can lead to pathological conditions (Semenza, 2007). Two processes, vasculogenesis and angiogenesis, are evident during normal vascular development. Because these processes are regulated by a complex interaction of signals, many chemicals can affect vascular development (Heldin, 2004; Taberero, 2007; Raffetto and Khalil, 2008).

Central nervous system (CNS) abnormalities caused by chemicals often involve insufficient or abnormal vascular development (Bardosi et al., 1985a,b, 1987; Hallene et al., 2006; Bassanini et al., 2007). Prenatal exposure to methylazoxymethanol acetate (MAM) in rats causes necrosis, loss of neurons, and disturbed neural progenitor migration in offspring (Haddad et al., 1972; Johnston and Coyle, 1979; Jones et al., 1981). Although the commonly accepted mechanism of action of MAM implicates the death of neural precursors (Cattaneo et al., 1995), some reports suggest that MAM-induced abnormalities include vascular malformations in the brain (Bardosi et al., 1985a,b, 1987). Results of a more recent study show that MAM neurotoxic activity in fetal rat brain is observed transiently (Bassanini et al.,

2007), but the inhibition of angiogenesis via decreased expression of vascular endothelial growth factor, aquaporin 1, and lectin B is persistent. Therefore, the occurrence of MAM-induced neural abnormalities depends on its dual action as a neurotoxin and an antiangiogenic factor. Recently, insufficient brain development caused by prenatal exposure to thalidomide, a well-known teratogen with potent antiangiogenic activity, was demonstrated to be caused by insufficient vascular development (Hallene et al., 2006). Neural development and vascular development share critical molecular signals during normal development (Yancopoulos et al., 1998). Although a close relationship between vascular development and neural development has been shown, the vascular toxicity of neurotoxins, other than MAM and thalidomide, remains unclear. Effects of prenatal exposure to permethrin on vascular development are also unknown in fetal brain and adult behavior.

Therefore, in this study, we examined the effects of prenatal exposure to permethrin on cerebral vascular development in mouse fetuses, CNS development, and on adult motor behavior later in life. Analysis of cerebral vascular development in the fetus brain was performed by anatomical and histochemical examination. CNS development was assessed by histochemical analysis and measurements of neurotransmitters in the juvenile brain of mice. Motor behaviors in adulthood were tested with a modified-SHIRPA screening.

MATERIALS AND METHODS

Animals and Chemical Administration

Animal protocols for the breeding and all other experiments were approved by NIES's Institutional Animal Care and Use Committee under the Guideline for Animal Care of NIES. ICR mice were purchased from CLEA Japan (Tokyo, Japan) and housed at a constant temperature ($22^{\circ}\text{C} \pm 0.5^{\circ}\text{C}$) at 35–70% humidity with 12-h light–dark photoperiod. Mice were given standard lsb chow and water *ad libitum*. At GD10.5, the pregnant mice were divided into seven groups of three to four mice per group and administered corn oil (Wako Pure Chemical Industries, Osaka, Japan) as the negative control and permethrin (Wako Pure Chemical Industries) at a dose of 2, 10, 50, or 75 mg/kg by oral gavage, which are 1/250, 1/50, 1/10, and 1/6.7 of the oral LD50 of mice (Miyamoto, 1976). For thalidomide (Wako Pure Chemical), a dose of 150 mg/kg was administered, respectively, at GD10.5. To determine the effects of permethrin on the development of cerebral arteries in the circle of Willis (CW), we conducted two experiments [Fig. 1(A,B)]. In the first experiment, anatomical and histological observations of cerebral arteries in the fetal mouse brain were examined at GD17.5. The second experiment investigated the later effects of prenatal exposure to

Abbreviations

ACA	anterior cerebral arteries
AComA	anterior communicating arteries
CW	circle of Willis
CNS	central nervous system
GD	gestation day
MAM	methylazoxymethanol acetate
MCA	middle cerebral artery
PFA	Paraformaldehyde

F1